AIMS Mathematics, 11(7): 20711–20745.
DOI: 10.3934/math.2026842
Received: 04 May 2026
Revised: 20 June 2026
Accepted: 29 June 2026
Published: 14 July 2026

https://www.aimspress.com/journal/Math

Research article

Fractional epidemic modeling of dengue: Sensitivity, stability, and bifurcation under environmental influence

Razia Sultana[1], **Md Rifat Hasan**[1,*], **Turki D. Alharbi**[2,*], **J. G. AL-Juaid**[3] **and M. T. Alharthi**[4]

[1] Department of Applied Mathematics, Faculty of Science, Noakhali Science and Technology University, Noakhali 3814, Bangladesh; raziasultana0081@gmail.com; rifatmathdu@gmail.com
[2] Department of Mathematics, Al-Leith University College, Umm Al-Qura University, Mecca 24381, Saudi Arabia; tdharbi@uqu.edu.sa
[3] Department of Mathematics and Statistics, College of Science, Taif University, P.O. Box 11099, Taif 21944, Saudi Arabia; jo.gh@tu.edu.sa
[4] Department of Mathematics, Applied College at Khulais, University of Jeddah, Jeddah 21589, Saudi Arabia; mtalharthi@uj.edu.sa

* **Correspondence:** Email: rifatmathdu@gmail.com, tdharbi@uqu.edu.sa.

Abstract: Dengue fever is a rapidly spreading vector-borne disease, posing severe health challenges worldwide due to its complex transmission dynamics between humans and mosquitoes. Traditional mathematical models often fail to capture memory effects and environmental influences that significantly affect disease progression. To address this, we formulated a fractional-order dengue transmission model incorporating environmental factors using the Caputo derivative. This approach allows the system dynamics to account for hereditary effects and delayed responses, providing a more realistic representation of dengue outbreaks. We analyzed the model's stability, bifurcation, and sensitivity, and conducted numerical simulations to examine how varying the fractional order and key epidemiological parameters impacts the disease dynamics. Our findings show that lower fractional orders slow the epidemic's progression, while higher orders approach classical integer-order behavior. The mosquito biting rate emerged as the most influential factor affecting the basic reproduction (R_0), whereas disease-induced human mortality had minimal impact. These results highlight critical parameters for controlling dengue's transmission and demonstrate that fractional-order models offer enhanced predictive power and insight compared with traditional models, supporting more effective public health interventions.

Keywords: dengue; fractional differential equation; bifurcation; Lyapunov; environment; sensitivity; stability
Mathematics Subject Classification: 34A08, 34D20, 34C60, 37G10, 92D30

1. Introduction

Dengue fever has become a major worldwide vector-borne disease and is rapidly becoming a threat to global public health [1]. Dengue is mainly transmitted through bites from infected female *Aedes aegypti* mosquitoes and has recently become the most common mosquito-borne diseases in the globe. The World Health Organization (WHO) reports that dengue has now become endemic in over 100 countries in Asia, Africa, North and South America, and the Western Pacific region with an estimated 390 million people are affected by the disease each year [2]. More than a million people are clinically infected [3]. Since no vaccines and no specific antiviral treatments have yet been developed, most prevention and control strategies focus on the control of mosquito populations. Many factors are responsible for the increasing number of dengue cases and the increasing range of locations where it occurs. Rapid urbanization and population growth, inadequate waste management, and changes in climate and rainfall patterns have created favorable breeding conditions for *Aedes aegypti* [4]. The combination of increased water storage, increased rain, and an increase in the temperature of mosquito breeding sites (the above mentioned conditions) creates a more favorable environment for Aedes mosquitoes [5]. In addition to this, human mobility and international travel contribute significantly to disease spread. The continued occurrence of two or more serotypes in a region increases the probability that the next infection will be severe. All of these factors make it even more important to continue to learn how dengue virus is transmitted. In response to the growing prevalence of dengue, mathematical modeling has emerged as a crucial tool for researching dengue's transmission and control. Mathematical models represent host and vector interactions in a single concise model that describes both biological and behavioral variables as well as demographic characteristics. Models can be used to predict future outbreaks, evaluate intervention strategies, and estimate the most critical epidemiological measurements.

Traditional compartmental models of disease progression such as the Susceptible, infected and recovered (SIR) model or susceptible, exposed, infected and recovered (SEIR) model, have been extensively used in this manner [6–9]. These models usually are described in terms of ordinary differential equations (ODEs) using integer-order derivatives, and they passively assume that the change rate in each compartment is solely dependent on the current system state. Although traditional integer-order models have been shown to be useful, they have inherent limitations. In particular, they lack an account for memory or history in their dynamics of disease transmission. Biological systems are often influenced by both present and past conditions. In many populations, the current state does not depend only on the individuals who are present at that time. It can also depend on people or organisms that were present earlier and were exposed to disease transmission. These past effects may continue through individuals who are still in the population, because of their earlier exposures or behaviours. They may also appear after a delay, as the system responds to earlier events. Examples include the incubation period of a disease, the time it take a person to gain or lose immunity, and the lifespan of mosquitoes can survive outside a host. Because of these factors, more flexible and general modeling approaches are needed to represent such biological complexity [10].

Fractional calculus deals with derivatives and integrals of non-integer order. It provides a useful alternative to classical calculus. In classical models, the current state of a system usually depends only on the present conditions. In fractional calculus, the present state can depend on the whole past history of the system. This feature is very useful in epidemiological modeling. In many diseases,

past events affect the present disease spread. For example, previous infections, delays in symptoms, immunity changes, and earlier interactions between humans and mosquitoes can influence the current situation. Among the different fractional derivatives, the Caputo derivative is widely used in real-world modeling [11, 12]. One reason is that it allows the use of standard initial conditions. It is also easier to handle mathematically compared with some other fractional derivatives. In recent years, fractional-order models have received more attention. These models can often fit real data better than traditional integer-order models. They can also describe complex epidemic patterns more clearly. For dengue fever, fractional models can be especially helpful. Dengue's transmission depends on the interaction between humans and mosquitoes [13, 14]. Since this interaction may involve memory effects and time delays, fractional models can give a better understanding of how the disease spreads and changes over time.

1.1. Literature review

Mathematical modeling has received an increasing amount of attention lately, with the public health implications and importance of epidemiology increasing as the study of dengue fever evolves over time. Historically, many early models for dengue (along with many other vector-borne diseases) were developed using systems of ODEs with an integer order that very simply approximated how the disease spread within a single population (either human or mosquitoes). Although these models provided a foundation for understanding these types of diseases, researchers soon identified a number of limitations of ODEs, particularly with storing history or heredity. This is now prompting a shift toward using more generalized fractional-order differential equations (FDE) methods.

Many significant research efforts have contributed to the advancement of mathematical models of dengue tranmission. Chowell et al. [15] and Shekhar [16] performed research on the dynamics of dengue using classical compartmetal models. These cases demonstrated that parameter sensitivity analysis and accurate prediction of anticipated outbreaks were critical features of their investigations into what has been referred to as dengue fever in the public health literature. The development of a global dengue risk map by Bhatt et al. [17] used spatial models. Brady et al. [18] also examined the risk associated with dengue and provided an estimate of risk population. Bancroft [19] was the first to provide evidence that mosquitoes were responsible for the transfer of the disease. The use of mathematical models to examine dengue control tactics (e.g., mosquito reduction and immunization) was also investigated by Rodrigues et al. [20] ultimately, through their use of statistical modeling. Historical evidence concerning the geographical spread of dengue has been reported by Halstead [21] and Kour et al. [22], who characterized the evolutionary shift from an endemic disease characterized by the absence of sustained transmission to an epidemic threat characterized by sustained transmission in the majority of regions of the world. Blaney et al. [23] studied dengue vaccine candidates through clinical trials. Alharbi et al. [24] developed a dengue model that includes hospitalized and symptomatic infected humans to study the disease's transmission, stability, and sensitivity. Many studies have also focused on collecting and analyzing dengue outbreak data. Shim [25] worked on age-structured models and time-series methods to study dengue's spread and control. Agusto and Khan [26] developed dengue models for the Khyber Pakhtunkhwa region of Pakistan.

Classical models are useful, but they have some limitations. In many cases, they cannot properly describe systems with memory effects. To solve this problem, researchers have started using fractional calculus. Fractional calculus extends normal derivatives and integrals to non-integer orders. The

basic theory of this method was developed by Samko et al. [27], Caputo and Fabrizio [28], and Atangana and Baleanu [29]. Atangana [30] applied fractional calculus to different disease models. Their results showed better data fitting and more accurate disease prediction. Khan et al. [31] developed a fractional-order dengue model for Pakistan using data from 2003 to 2015. Verma et al. [32] developed a combined SIR-SI model to study dengue transmission between humans and mosquitoes, and extended it using fractional-order derivatives to include memory effects in the spread of the disease. Harjule et al. [33] proposed a hybrid SEISRD-SI dengue model using both classical and fractional-order dynamics, including severe dengue and dengue-induced death compartments to better describe disease transmission. Vijayalakshmi and Ariyanatchi [34] developed a fractional-order mathematical model to study mosquito populations with and without Wolbachia infection and their effect on dengue transmission. Another study [35] proposed a fractional-order dengue model using the Atangana–Baleanu–Caputo derivative to include memory effects, reinfection, and antibody-dependent enhancement in disease transmission. Olayiwola et al. [36] developed a Caputo fractional-order within-host dengue model to analyze the interaction among susceptible monocytes, infected monocytes, free dengue particles, and immune cells under adaptive immune responses. Sk et al. [37] developed a single-strain fractional-order dengue model based on stochastic processes, incorporating fractional transmission and recovery to study disease-free and endemic stability using R_0. Another study [38] examined dengue transmission using a fractional-order model by comparing disease spread with and without public awareness among the host population. A recent publication by Dave et al. [39] described a new approach to modeling the transmission of dengue fever using a fractional-order SEIR-SEI model and applying the Atangana-Baleanu fractional derivative to account for memory effects in both mosquito and human populations. Traore et al. [40] studied a Caputo fractional-order model to determine how memory effects influence the long-term behavior of a disease. Ahmad et al. [41] investigated a fractional-order human immunodeficiency virus/acquired immunodeficiency syndrome(HIV/AIDS) epidemic model under the Caputo operator and analyzed its global stability and computational behavior. Recent studies have emphasized the importance of convergence, accuracy, and error analysis in numerical simulations of fractional-order models. Khader et al. [42] developed a spectral collocation method based on Appell-type Changhee polynomials for fractional RLC electrical circuit models and used residual error analysis to examine their numerical accuracy. Similarly, Khader and Adel [43] applied fractional Bernoulli functions to a crossover lumpy skin disease model under the Liouville–Caputo fractional derivative and discussed the convergence analysis for the proposed approximation method. Abdelmonem [44] investigated a dual nonlinear saturation control strategy for an electromagnetic suspension system in maglev trains, demonstrating the relevance of advanced stability and control methods in nonlinear mathematical models.

Overall, these studies show the development of dengue modeling over time. Earlier studies mainly used classical integer-order models. Later studies introduced fractional-order models and more detailed compartmental structures. These advanced models can describe dengue transmission more realistically because they include memory, immunity delay, and behavioral changes. These factors are very important for long-lasting vector-borne diseases like dengue.

1.2. Novelty and contributions of the present study

We present a new understanding of dengue modeling in this work, integrating the effects of the environment with the work of fractional-order calculus to provide a more detailed and realistic

representation of the dynamics of the disease. Our model incorporates the effects of memory and heredity by using the Caputo fractional derivative to determine how past infection and exposure affect the current patterns of infection transmission. The model incorporates environmental factors that influence the mosquito population's growth and consequently affect dengue transmission. This environmental index reflects favorable ecological conditions for mosquito breeding and survival, including water accumulation, humidity levels, and breeding site availability. We determine the most significant drivers of dengue transmission, including the mosquito biting rates, through stability, bifurcation, and sensitivity analyses and investigate how the parameter of the fractional-order alpha can change the speed and strength of epidemics. This combination method not only increases our knowledge about the transmission of dengue but also offers some practical insights on how to design effective public health interventions that fill the gap between theory and practice in the control of dengue epidemics.

1.3. Organization of the study

The rest of this paper is structured in the following way. In Section 2, we develop a mathematical model dividing the human and mosquito populations into epidemiologically useful compartments with the addition of environmental viral load. In Section 3, the theoretical analyses are provided for the properties of the model, such as the derivation of R_0, and the existence of equilibria with their stability analysis in Section 4. In Section 5, we carry out a bifurcation analysis of multiple equilibria. The sensitivity analysis of R_0 is given in Section 6, and Section 7 discusses the numerical studies which were used to demonstrate and prove the analytical findings. Finally, Section 8 summarizes the paper with the major findings and recommendations for effective public health interventions against dengue.

2. Formulation of the dengue model

Comprehending the trends of infectious disease dissemination is a critical step to prevent their emergence and to control outbreaks. One of the principal tools for achieving this is the mathematical modeling of disease dynamics through systems of ODEs or partial differential equations. Properly capturing the spread of processes between species that interact allows the current analytical approaches to produce strong findings with significant biological significance.

In this section, we formulate a fractional-order dengue transmission model that incorporates the effect of environmental factors on mosquito recruitment and disease propagation. The human population at time t is divided into three epidemiological classes: Susceptible humans $S_H(t)$, infected humans $I_H(t)$, and recovered humans $R_H(t)$. Similarly, the mosquito population is divided into susceptible mosquitoes $S_V(t)$ and infected mosquitoes $I_V(t)$. In addition, we introduce an environmental state variable $E_V(t)$. It represents ecological conditions that favor mosquitoes' breeding and survival, such as accumulated rainfall, stagnant water, humidity, and the availability of breeding sites. Accordingly, the total human and mosquito populations are given by

$$N_H(t) = S_H(t) + I_H(t) + R_H(t), \qquad N_V(t) = S_V(t) + I_V(t). \tag{2.1}$$

Under these assumptions, the dengue model is described by the following system of Caputo fractional differential equations:

$$
\begin{aligned}
{}^{C}D_t^{\alpha} S_H(t) &= \Lambda_H - b_V \beta_H S_H(t) I_V(t) - \mu_H S_H(t), \\
{}^{C}D_t^{\alpha} I_H(t) &= b_V \beta_H S_H(t) I_V(t) - (\delta_H + \gamma_H + \mu_H) I_H(t), \\
{}^{C}D_t^{\alpha} R_H(t) &= \gamma_H I_H(t) - \mu_H R_H(t), \\
{}^{C}D_t^{\alpha} S_V(t) &= \Lambda_V + \omega E_V(t) - b_V \beta_V S_V(t) I_H(t) - \mu_V S_V(t), \\
{}^{C}D_t^{\alpha} I_V(t) &= b_V \beta_V S_V(t) I_H(t) - \mu_V I_V(t), \\
{}^{C}D_t^{\alpha} E_V(t) &= k I_V(t) - \xi E_V(t),
\end{aligned}
\tag{2.2}
$$

where $0 < \alpha \leq 1$ denotes the fractional order in the Caputo sense.

The model parameters are interpreted as follows. The quantity Λ_H denotes the recruitment rate of humans into the susceptible class, while μ_H represents the natural death rate of humans. Susceptible humans become infected through effective contact with infected mosquitoes at the rate $b_V \beta_H S_H I_V$, where b_V is the mosquito biting rate and β_H is the transmission coefficient from infected mosquitoes to susceptible humans. Infected humans recover at the rate γ_H, die due to dengue at the rate δ_H, and are also subject to natural death at the rate μ_H.

For the mosquito population, Λ_V is the baseline recruitment rate of mosquitoes and μ_V is the natural mortality rate of mosquitoes. Susceptible mosquitoes acquire an infection after contact with infected humans at the rate $b_V \beta_V S_V I_H$, where β_V denotes the transmission coefficient from infected humans to susceptible mosquitoes. The environmental variable $E_V(t)$ contributes positively to mosquito recruitment through the term $\omega E_V(t)$, where ω measures the strength of environmental influence on mosquito growth. Moreover, the environmental component is assumed to increase in proportion to the infected mosquito population at the rate $kI_V(t)$ and to decay naturally at the rate $\xi E_V(t)$.

The use of the Caputo fractional derivative allows the model to account for memory and hereditary effects in dengue transmission dynamics. This is biologically relevant because the present progression of infection and vector abundance may depend not only on the current population levels but also on their past states. Therefore, the fractional framework provides a more flexible and realistic description of dengue dynamics than the corresponding integer-order model when delayed environmental and epidemiological effects are important.

For convenience, the Caputo fractional derivative of order $\alpha \in (0, 1]$ is defined by

$$
{}^{C}D_t^{\alpha} f(t) = \frac{1}{\Gamma(1-\alpha)} \int_0^t \frac{f'(s)}{(t-s)^{\alpha}} \, ds, \qquad 0 < \alpha < 1, \tag{2.3}
$$

where $\Gamma(\cdot)$ denotes the gamma function.

The model (2.2) is based on the following assumptions:

1. The human population is divided into susceptible, infected, and recovered classes, whereas the mosquito population is divided into susceptible and infected classes.
2. The recruitment rates of humans and mosquitoes are constant and given by Λ_H and Λ_V, respectively.
3. Transmission occurs through homogeneous mixing between humans and mosquitoes.
4. Recovered humans acquire immunity during the time interval under consideration.
5. Mosquitoes do not recover from infection.
6. The environmental variable $E_V(t)$ does not directly cause infection, but indirectly affects disease dynamics through mosquito recruitment.

7. The environmental effect increases with infected mosquitoes and decays naturally over time.
8. Vertical transmission and the immigration of infected individuals or mosquitoes are neglected.

For clarity, the notation used in Model (2.2) is summarized in Table 1 and Figure 1 .

Table 1. Description of state variables and parameters used in the dengue model.

Symbol	Description
$S_H(t)$	Susceptible human population
$I_H(t)$	Infected human population
$R_H(t)$	Recovered human population
$S_V(t)$	Susceptible mosquito population
$I_V(t)$	Infected mosquito population
$E_V(t)$	Environmental factor influencing mosquito recruitment
Λ_H	Human recruitment rate
Λ_V	Baseline mosquito recruitment rate
b_V	Mosquito biting rate
β_H	Transmission coefficient from mosquitoes to humans
β_V	Transmission coefficient from humans to mosquitoes
μ_H	Natural death rate of humans
μ_V	Natural death rate of mosquitoes
γ_H	Recovery rate of infected humans
δ_H	Disease-induced death rate of infected humans
ω	Environmental contribution rate to mosquito recruitment
k	Rate at which infected mosquitoes enhance the environmental effect
ξ	Natural depletion rate of environmental influence
α	Fractional order of the Caputo derivative

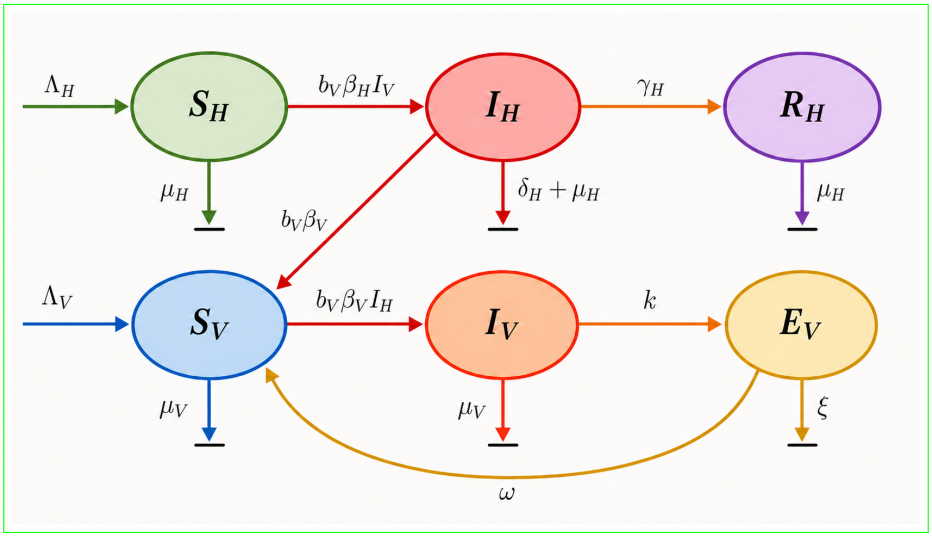

Figure 1. Transmission of the dengue virus.

3. Dengue model analyses

3.1. Existence of the unique non-negative solution

We now prove that the system admits a unique solution that remains non-negative for all $t > 0$, provided that the initial conditions are non-negative. To do this, we apply standard results from the theory of fractional differential equations using Caputo derivatives.

Let us denote the solution vector as

$$R_+^6 = \{x(t) \in \mathbb{R}^6 \mid x(t) \geq 0\}, \quad x(t) = \left(S_H(t), I_H(t), R_H(t), S_V(t), I_V(t), E_V(t)\right)^t. \tag{3.1}$$

We follow the method used in [45] and provide the following results.

Lemma 1. *Consider $u(x) \in C[a, b]$ and ${}^C D_t^\alpha u(x) \in (a, b]$. Then*

$$u(t) = u(a) + \frac{1}{\Gamma(\alpha)}({}^C D_a^\alpha u)(\tau)(t-a)^\alpha, \quad a \leq \tau \leq t, \quad \forall t \in (a, b].$$

Corollary 1 ([46])**.** *Consider $u(x) \in C[a, b]$ and ${}^C D_t^\alpha u(x) \in (a, b]$, where $\alpha \in (0, 1]$. Then the following holds*

- *If ${}^C D_t^\alpha u \geq 0$ for all $a < x < b$, then $u(x)$ is non-decreasing.*
- *If ${}^C D_t^\alpha u \leq 0$ for all $a < x < b$, then $u(x)$ is non-increasing.*

3.2. Positivity and the boundedness of solutions

In this subsection, we prove that the solutions of System (2.2) remain biologically meaningful. That is, for non-negative initial conditions, all state variables remain non-negative and bounded for all $t \geq 0$.

Let

$$X(t) = (S_H(t), I_H(t), R_H(t), S_V(t), I_V(t), E_V(t))^T$$

and define the non-negative region as

$$\mathbb{R}_+^6 = \left\{X(t) \in \mathbb{R}^6 : S_H, I_H, R_H, S_V, I_V, E_V \geq 0\right\}.$$

Theorem 3.1. *For any initial condition*

$$X(0) \in \mathbb{R}_+^6,$$

the solution of the fractional dengue model Eq (2.2) remains non-negative for all $t \geq 0$.

Proof. We show that the vector field points inward on each boundary of $\mathbb{R}_+^6$. From System (2.2), we have

$${}^C D_t^\alpha S_H = \Lambda_H - b_V \beta_H S_H I_V - \mu_H S_H.$$

If $S_H = 0$, then

$${}^C D_t^\alpha S_H\Big|_{S_H=0} = \Lambda_H \geq 0.$$

Similarly

$${}^C D_t^\alpha I_H = b_V \beta_H S_H I_V - (\delta_H + \gamma_H + \mu_H) I_H.$$

If $I_H = 0$, then

$$^{C}D_t^{\alpha} I_H\big|_{I_H=0} = b_V \beta_H S_H I_V \geq 0.$$

Moreover

$$^{C}D_t^{\alpha} R_H = \gamma_H I_H - \mu_H R_H.$$

If $R_H = 0$, then

$$^{C}D_t^{\alpha} R_H\big|_{R_H=0} = \gamma_H I_H \geq 0.$$

For susceptible mosquitoes we have

$$^{C}D_t^{\alpha} S_V = \Lambda_V + \omega E_V - b_V \beta_V S_V I_H - \mu_V S_V.$$

If $S_V = 0$, then

$$^{C}D_t^{\alpha} S_V\big|_{S_V=0} = \Lambda_V + \omega E_V \geq 0.$$

For infected mosquitoes we have

$$^{C}D_t^{\alpha} I_V = b_V \beta_V S_V I_H - \mu_V I_V.$$

If $I_V = 0$, then

$$^{C}D_t^{\alpha} I_V\big|_{I_V=0} = b_V \beta_V S_V I_H \geq 0.$$

Finally, for the environmental variable we have

$$^{C}D_t^{\alpha} E_V = kI_V - \xi E_V.$$

If $E_V = 0$, then

$$^{C}D_t^{\alpha} E_V\big|_{E_V=0} = kI_V \geq 0.$$

Thus, the Caputo derivative of each variable is non-negative whenever that variable reaches zero. By the generalized comparison principle for Caputo fractional differential equations, no solution starting in $\mathbb{R}^6_+$ can cross the boundary of $\mathbb{R}^6_+$. Hence we have

$$X(t) \in \mathbb{R}^6_+, \qquad t \geq 0.$$

This proves the positivity. □

Next, we prove the boundedness.

Let the total human population be

$$N_H(t) = S_H(t) + I_H(t) + R_H(t).$$

Adding the first three equations of System (2.2), we obtain

$$^{C}D_t^{\alpha} N_H = \Lambda_H - \mu_H S_H - (\delta_H + \mu_H) I_H - \mu_H R_H.$$

Therefore

$$^{C}D_t^{\alpha} N_H = \Lambda_H - \mu_H N_H - \delta_H I_H.$$

Since $\delta_H I_H \geq 0$, it follows that

$$^{C}D_t^{\alpha} N_H \leq \Lambda_H - \mu_H N_H.$$

By the fractional comparison theorem we have

$$N_H(t) \leq N_H(0)E_{\alpha}(-\mu_H t^{\alpha}) + \frac{\Lambda_H}{\mu_H}\left[1 - E_{\alpha}(-\mu_H t^{\alpha})\right],$$

where $E_{\alpha}(\cdot)$ is the Mittag–Leffler function. Hence we have

$$\limsup_{t\to\infty} N_H(t) \leq \frac{\Lambda_H}{\mu_H}.$$

Thus, the human population is bounded.

Now let

$$N_V(t) = S_V(t) + I_V(t)$$

be the total mosquito population. Adding the mosquito equations gives

$$^{C}D_t^{\alpha} N_V = \Lambda_V + \omega E_V - \mu_V N_V.$$

Moreover

$$^{C}D_t^{\alpha} E_V = kI_V - \xi E_V.$$

Since $I_V \leq N_V$, we have

$$^{C}D_t^{\alpha} E_V \leq kN_V - \xi E_V.$$

To prove boundedness of the coupled mosquito-environment subsystem, we assume the environmental dissipation condition

$$\mu_V \xi > k\omega.$$

Then a positive constant c exists such that

$$\frac{\omega}{\xi} < c < \frac{\mu_V}{k}.$$

Define

$$W(t) = N_V(t) + cE_V(t).$$

Then

$$\begin{aligned} ^{C}D_t^{\alpha} W &= {}^{C}D_t^{\alpha} N_V + c\,{}^{C}D_t^{\alpha} E_V \\ &\leq \Lambda_V + \omega E_V - \mu_V N_V + c(kN_V - \xi E_V) \\ &= \Lambda_V - (\mu_V - ck)N_V - (c\xi - \omega)E_V. \end{aligned}$$

Since

$$\mu_V - ck > 0 \qquad \text{and} \qquad c\xi - \omega > 0,$$

choose

$$\eta = \min\left\{\mu_V - ck,\ \frac{c\xi - \omega}{c}\right\} > 0.$$

Then

$$^{C}D_t^{\alpha} W \leq \Lambda_V - \eta W.$$

Again, using the fractional comparison theorem we have

$$W(t) \leq W(0)E_\alpha(-\eta t^\alpha) + \frac{\Lambda_V}{\eta}\left[1 - E_\alpha(-\eta t^\alpha)\right].$$

Therefore

$$\limsup_{t\to\infty} W(t) \leq \frac{\Lambda_V}{\eta}.$$

Since

$$N_V(t) \leq W(t), \qquad E_V(t) \leq \frac{W(t)}{c},$$

it follows that $N_V(t)$ and $E_V(t)$ are bounded. Hence we have

$$S_V(t), I_V(t), E_V(t)$$

are bounded for all $t \geq 0$.

Combining the human and mosquito-environment estimates, all state variables of System (2.2) remain non-negative and bounded in the feasible region

$$\Omega = \left\{X \in \mathbb{R}^6_+ : N_H(t) \leq \frac{\Lambda_H}{\mu_H}, \quad N_V(t) + cE_V(t) \leq \frac{\Lambda_V}{\eta}\right\},$$

where

$$\eta = \min\left\{\mu_V - ck, \frac{c\xi - \omega}{c}\right\} > 0.$$

Thus, Ω is positively invariant and attracting for System (2.2).

3.3. Model equilibria

We obtain the model equilibria for the fractional dengue model (2.2) by setting

$${}^C D_t^\alpha S_H = {}^C D_t^\alpha I_H = {}^C D_t^\alpha R_H = {}^C D_t^\alpha S_V = {}^C D_t^\alpha I_V = {}^C D_t^\alpha E_V = 0. \tag{3.2}$$

The fractional dengue model possesses the following two equilibrium points.

3.3.1. Disease-free equilibrium

The disease-free equilibrium (DFE) is given by

$$E_0 = \left(\frac{\Lambda_H}{\mu_H}, 0, 0, \frac{\Lambda_V}{\mu_V}, 0, 0\right). \tag{3.3}$$

3.3.2. Endemic equilibrium

Let

$$E_1^* = (S_H^*, I_H^*, R_H^*, S_V^*, I_V^*, E_V^*)$$

denote the endemic equilibrium(EE) of System (2.2). For simplicity, define

$$A_H = \delta_H + \gamma_H + \mu_H, \qquad a_H = b_V\beta_H, \qquad a_V = b_V\beta_V.$$

At the EE, all Caputo derivatives are zero. Therefore,

$$0 = \Lambda_H - a_H S_H^* I_V^* - \mu_H S_H^*,$$

$$0 = a_H S_H^* I_V^* - A_H I_H^*,$$

$$0 = \gamma_H I_H^* - \mu_H R_H^*,$$

$$0 = \Lambda_V + \omega E_V^* - a_V S_V^* I_H^* - \mu_V S_V^*,$$

$$0 = a_V S_V^* I_H^* - \mu_V I_V^*,$$

and

$$0 = k I_V^* - \xi E_V^*.$$

From these equations, we obtain

$$S_H^* = \frac{\Lambda_H}{\mu_H + a_H I_V^*},$$

$$I_H^* = \frac{a_H S_H^* I_V^*}{A_H},$$

$$R_H^* = \frac{\gamma_H I_H^*}{\mu_H},$$

and

$$E_V^* = \frac{k I_V^*}{\xi}.$$

Now define

$$\Delta = a_H a_V \Lambda_H \Lambda_V - \mu_H \mu_V^2 A_H.$$

Using the expression of the basic reproduction number,

$$R_0^2 = \frac{a_H a_V \Lambda_H \Lambda_V}{\mu_H \mu_V^2 A_H},$$

we can write

$$\Delta = \mu_H \mu_V^2 A_H (R_0^2 - 1).$$

We also define

$$B = \mu_V^2 A_H \xi + a_V \Lambda_H (\mu_V \xi - k\omega),$$

and

$$C = \mu_H (\mu_V \xi - k\omega) + \xi a_H \Lambda_V.$$

Then the EE is given by

$$E_1^* = \left(\frac{B}{a_V C}, \frac{\xi \Delta}{A_H a_V C}, \frac{\gamma_H \xi \Delta}{\mu_H A_H a_V C}, \frac{\mu_V A_H C}{a_H B}, \frac{\xi \Delta}{a_H B}, \frac{k \Delta}{a_H B} \right).$$

The EE exists if $R_0 > 1$ and $\mu_V \xi > k\omega$.

3.4. Basic reproduction number R_0

We obtain R_0 using the next-generation matrix method. Let

$$F = \begin{bmatrix} \text{new infections in } I_H \\ \text{new infections in } I_V \\ \text{new infections in } E_V \end{bmatrix} \quad \Rightarrow \quad F = \begin{bmatrix} \frac{\partial(b_V\beta_H S_H I_V)}{\partial I_H} & \frac{\partial(b_V\beta_H S_H I_V)}{\partial I_V} & \frac{\partial(b_V\beta_H S_H I_V)}{\partial E_V} \\ \frac{\partial(b_V\beta_V S_V I_H)}{\partial I_H} & \frac{\partial(b_V\beta_V S_V I_H)}{\partial I_V} & \frac{\partial(b_V\beta_V S_V I_H)}{\partial E_V} \\ 0 & 0 & 0 \end{bmatrix} = \begin{bmatrix} 0 & b_V\beta_H S_H & 0 \\ b_V\beta_V S_V & 0 & 0 \\ 0 & 0 & 0 \end{bmatrix}.$$

Similarly, the transition matrix is

$$V = \begin{bmatrix} \delta_H + \gamma_H + \mu_H & 0 & 0 \\ 0 & \mu_V & 0 \\ 0 & -k & \xi \end{bmatrix}.$$

Its inverse is

$$V^{-1} = \begin{bmatrix} \frac{1}{\delta_H+\gamma_H+\mu_H} & 0 & 0 \\ 0 & \frac{1}{\mu_V} & 0 \\ 0 & \frac{k}{\xi\mu_V} & \frac{1}{\xi} \end{bmatrix}.$$

Then the next-generation matrix is

$$FV^{-1} = \begin{bmatrix} 0 & \frac{b_V\beta_H S_H}{\delta_H+\gamma_H+\mu_H} & 0 \\ \frac{b_V\beta_V S_V}{\mu_V} & 0 & 0 \\ \frac{kb_V\beta_V S_V}{\xi\mu_V} & 0 & 0 \end{bmatrix}.$$

At the DFE $S_H = \Lambda_H/\mu_H$, $S_V = \Lambda_V/\mu_V$, the matrix becomes

$$A = FV^{-1} = \begin{bmatrix} 0 & \frac{b_V\beta_H\Lambda_H}{\mu_H(\delta_H+\gamma_H+\mu_H)} & 0 \\ \frac{b_V\beta_V\Lambda_V}{\mu_V^2} & 0 & 0 \\ \frac{kb_V\beta_V\Lambda_V}{\xi\mu_V^2} & 0 & 0 \end{bmatrix}.$$

The characteristic equation is

$$\det(A - \lambda I) = \begin{vmatrix} -\lambda & \frac{b_V\beta_H\Lambda_H}{\mu_H(\delta_H+\gamma_H+\mu_H)} & 0 \\ \frac{b_V\beta_V\Lambda_V}{\mu_V^2} & -\lambda & 0 \\ \frac{kb_V\beta_V\Lambda_V}{\xi\mu_V^2} & 0 & -\lambda \end{vmatrix} = 0 \quad \Rightarrow \quad \lambda^2 - \frac{b_V^2\beta_V\beta_H\Lambda_V\Lambda_H}{\mu_H\mu_V^2(\delta_H + \gamma_H + \mu_H)} = 0.$$

Hence, the R_0 is

$$R_0 = \sqrt{\frac{b_V^2\beta_V\beta_H\Lambda_V\Lambda_H}{\mu_H\mu_V^2(\delta_H + \gamma_H + \mu_H)}}. \tag{3.4}$$

4. Stability analysis

4.1. Local stability of E_0

To prove the local stability of the fractional dengue model (2.2), the DFE is

$$E_0 = \left(\frac{\Lambda_H}{\mu_H}, 0, 0, \frac{\Lambda_V}{\mu_V}, 0, 0\right),$$

and the Jacobian matrix is

$$J(E_0) = \begin{bmatrix} -\mu_H & 0 & 0 & 0 & -b_V\beta_H & 0 \\ 0 & -(\delta_H + \gamma_H + \mu_H) & 0 & 0 & b_V\beta_H & 0 \\ 0 & \gamma_H & -\mu_H & 0 & 0 & 0 \\ 0 & -\frac{\mu_H b_V \beta_V \Lambda_V}{\Lambda_H \mu_V} & 0 & -\mu_V & 0 & \omega \\ 0 & \frac{\mu_H b_V \beta_V \Lambda_V}{\Lambda_H \mu_V} & 0 & 0 & -\mu_V & 0 \\ 0 & 0 & 0 & 0 & k & -\xi \end{bmatrix}.$$

The eigenvalues are

$$\lambda_1 = -\mu_H, \quad \lambda_2 = -\mu_H, \quad \lambda_3 = -\mu_V, \quad \lambda_4 = -\xi.$$

For the 2×2 subsystem

$$J = \begin{bmatrix} -(\delta_H + \gamma_H + \mu_H) & b_V\beta_H \\ \frac{\mu_H b_V \beta_V \Lambda_V}{\Lambda_H \mu_V} & -\mu_V \end{bmatrix},$$

the characteristic equation is

$$\lambda^2 + \lambda(\delta_H + \gamma_H + \mu_H + \mu_V) + \mu_V(\delta_H + \gamma_H + \mu_H)(1 - R_0^2) = 0,$$

$$\lambda^2 + a_1\lambda + a_0 = 0$$

where

$$a_1 = (\delta_H + \gamma_H + \mu_H + \mu_V),$$

which is always positive, and

$$a_0 = \mu_V(\delta_H + \gamma_H + \mu_H)(1 - R_0^2).$$

Now, two cases arise.

- If $R_0 < 1$, then $a_0 > 0$. Since both coefficients a_1 and a_0 are positive, both eigenvalues have negative real parts. Therefore, the DFE is locally asymptotically stable.
- If $R_0 > 1$, then $a_0 < 0$, which implies that the two eigenvalues have opposite signs. Hence, one eigenvalue is positive and the DFE becomes unstable, indicating the possibility of an epidemic outbreak.

4.2. Global stability of the DFE E_0

Theorem 4.1. *The fractional dengue model* (2.2) *with an arbitrary fractional order* $\alpha \in (0, 1]$ *is globally asymptotically stable at* E_0 *if* $\mu_V\xi > k\omega$ *and* $R_0 < 1$.

Proof.

$$\mathcal{L}(t) = \phi_1\left(S_H - S_H^0 - S_H^0 \ln\frac{S_H}{S_H^0}\right) + \phi_2 I_H$$
$$+ \phi_3\left(S_V - S_V^0 - S_V^0 \ln\frac{S_V}{S_V^0}\right) + \phi_4 I_V + \phi_5 E_V,$$

where $\phi_i > 0$ for $i = 1, 2, 3, 4, 5$. Using the Caputo fractional inequality for Volterra-type Lyapunov functions, we obtain

$$
\begin{aligned}
{}^{C}D_t^{\alpha}\mathcal{L}(t) \leq \phi_1\left(1 - \frac{S_H^0}{S_H}\right){}^{C}D_t^{\alpha}S_H + \phi_2{}^{C}D_t^{\alpha}I_H \\
+ \phi_3\left(1 - \frac{S_V^0}{S_V}\right){}^{C}D_t^{\alpha}S_V + \phi_4{}^{C}D_t^{\alpha}I_V + \phi_5{}^{C}D_t^{\alpha}E_V.
\end{aligned}
$$

Substituting the model equations gives

$$
\begin{aligned}
{}^{C}D_t^{\alpha}\mathcal{L}(t) \leq & -\phi_1\mu_H\frac{(S_H - S_H^0)^2}{S_H} - \phi_3\mu_V\frac{(S_V - S_V^0)^2}{S_V} \\
& + a_H(\phi_2 - \phi_1)S_HI_V + a_V(\phi_4 - \phi_3)S_VI_H \\
& + \left(\phi_3a_VS_V^0 - \phi_2A_H\right)I_H \\
& + \left(\phi_1a_HS_H^0 - \phi_4\mu_V + \phi_5k\right)I_V \\
& + \left[\phi_3\omega\left(1 - \frac{S_V^0}{S_V}\right) - \phi_5\xi\right]E_V.
\end{aligned}
$$

Now choose

$$\phi_1 = \phi_2 = m > 0, \qquad \phi_4 = \phi_3,$$

and

$$\phi_5 = \frac{\phi_3\omega}{\xi}.$$

Then

$$a_H(\phi_2 - \phi_1)S_HI_V = 0$$

and

$$a_V(\phi_4 - \phi_3)S_VI_H = 0.$$

Therefore

$$
\begin{aligned}
{}^{C}D_t^{\alpha}\mathcal{L}(t) \leq & -m\mu_H\frac{(S_H - S_H^0)^2}{S_H} - \phi_3\mu_V\frac{(S_V - S_V^0)^2}{S_V} \\
& - \left(mA_H - \phi_3a_VS_V^0\right)I_H \\
& - \left[\phi_3\left(\mu_V - \frac{k\omega}{\xi}\right) - ma_HS_H^0\right]I_V \\
& - \frac{\phi_3\omega S_V^0}{S_V}E_V.
\end{aligned}
$$

To ensure that all coefficients are positive, we choose ϕ_3 such that

$$\frac{ma_HS_H^0}{\mu_V - \frac{k\omega}{\xi}} < \phi_3 < \frac{mA_H}{a_VS_V^0}.$$

Such a positive ϕ_3 exists if and only if

$$\frac{a_H a_V S_H^0 S_V^0}{A_H\left(\mu_V - \frac{k\omega}{\xi}\right)} < 1,$$

which is equivalent to

$$\mathcal{R}_0 < 1, \quad \text{when } \mu_V \xi > k\omega.$$

Hence

$${}^C D_t^\alpha \mathcal{L}(t) \leq 0.$$

Moreover

$${}^C D_t^\alpha \mathcal{L}(t) = 0$$

holds only when

$$S_H = S_H^0, \qquad S_V = S_V^0, \qquad I_H = 0, \qquad I_V = 0, \qquad E_V = 0.$$

Therefore, the largest invariant set contained in

$$\left\{x \in \mathbb{R}_+^6 : {}^C D_t^\alpha \mathcal{L}(t) = 0\right\}$$

is exactly

$$E_0 = \left(S_H^0, 0, 0, S_V^0, 0, 0\right).$$

By the fractional Lyapunov–LaSalle invariance principle for Caputo fractional-order systems, the DFE E_0 is globally asymptotically stable whenever

$$\mathcal{R}_0 < 1, \qquad \mu_V \xi > k\omega.$$

□

4.3. Global stability of E_1^*

Theorem 4.2. *If $R_0 > 1$, then the fractional dengue model* (2.2) *at E_1^* is globally asymptotically stable.*

Proof. We consider the following Lyapunov function:

$$\begin{aligned} L(t) = {} & \rho_1\Big(S_H - S_H^* - S_H^* \ln \frac{S_H}{S_H^*}\Big) + \rho_2\Big(I_H - I_H^* - I_H^* \ln \frac{I_H}{I_H^*}\Big) + \rho_3\Big(S_V - S_V^* - S_V^* \ln \frac{S_V}{S_V^*}\Big) \\ & + \rho_4\Big(I_V - I_V^* - I_V^* \ln \frac{I_V}{I_V^*}\Big) + \rho_5\Big(E_V - E_V^* - E_V^* \ln \frac{E_V}{E_V^*}\Big). \end{aligned} \tag{4.1}$$

Using the Caputo fractional inequality, we obtain

$$\begin{aligned} {}^C D_t^\alpha L(t) \leq {} & \rho_1\Big(1 - \frac{S_H^*}{S_H}\Big){}^C D_t^\alpha S_H + \rho_2\Big(1 - \frac{I_H^*}{I_H}\Big){}^C D_t^\alpha I_H \\ & + \rho_3\Big(1 - \frac{S_V^*}{S_V}\Big){}^C D_t^\alpha S_V + \rho_4\Big(1 - \frac{I_V^*}{I_V}\Big){}^C D_t^\alpha I_V + \rho_5\Big(1 - \frac{E_V^*}{E_V}\Big){}^C D_t^\alpha E_V. \end{aligned}$$

For convenience, introduce the normalized variables

$$x = \frac{S_H}{S_H^*}, \qquad y = \frac{I_H}{I_H^*}, \qquad z = \frac{S_V}{S_V^*}, \qquad w = \frac{I_V}{I_V^*}, \qquad u = \frac{E_V}{E_V^*}.$$

Now, using the model equations and the EE identities, we obtain

$$\left(1 - \frac{S_H^*}{S_H}\right) {}^C D_t^\alpha S_H = -\mu_H S_H^* \frac{(x-1)^2}{x} + \Lambda_H I_H^* \left(1 - \frac{1}{x} - xw + w\right),$$

$$\left(1 - \frac{I_H^*}{I_H}\right) {}^C D_t^\alpha I_H = \Lambda_H I_H^* \left(xw + 1 - y - \frac{xw}{y}\right),$$

$$\left(1 - \frac{S_V^*}{S_V}\right) {}^C D_t^\alpha S_V = -\mu_V S_V^* \frac{(z-1)^2}{z} + \mu_V I_V^* \left(1 - \frac{1}{z} - zy + y\right) + \omega E_V^* (u-1)\left(1 - \frac{1}{z}\right),$$

$$\left(1 - \frac{I_V^*}{I_V}\right) {}^C D_t^\alpha I_V = \mu_V I_V^* \left(zy + 1 - w - \frac{zy}{w}\right),$$

and

$$\left(1 - \frac{E_V^*}{E_V}\right) {}^C D_t^\alpha E_V = \xi E_V^* \left(w + 1 - u - \frac{w}{u}\right).$$

Choose

$$\rho_1 = \rho_2 = \rho_H > 0, \qquad \rho_3 = \rho_4 = \rho_V > 0,$$

such that

$$\rho_H \Lambda_H I_H^* = \rho_V \mu_V I_V^*.$$

For example, one may take

$$\rho_1 = \rho_2 = \mu_V I_V^*, \qquad \rho_3 = \rho_4 = \Lambda_H I_H^*.$$

Let

$$P = \rho_H \Lambda_H I_H^* = \rho_V \mu_V I_V^*.$$

Then the host–vector infection cross-terms reduce to

$$P\left[4 - \frac{1}{x} - \frac{1}{z} - \frac{xw}{y} - \frac{zy}{w}\right].$$

Since

$$\frac{1}{x} \cdot \frac{1}{z} \cdot \frac{xw}{y} \cdot \frac{zy}{w} = 1,$$

the arithmetic–geometric mean inequality gives

$$\frac{1}{x} + \frac{1}{z} + \frac{xw}{y} + \frac{zy}{w} \geq 4.$$

Therefore

$$P\left[4 - \frac{1}{x} - \frac{1}{z} - \frac{xw}{y} - \frac{zy}{w}\right] \leq 0.$$

Consequently

$$
\begin{aligned}
{}^{C}D_t^{\alpha} L(t) \leq & -\rho_H \mu_H S_H^* \frac{(x-1)^2}{x} - \rho_V \mu_V S_V^* \frac{(z-1)^2}{z} \\
& + P\left[4 - \frac{1}{x} - \frac{1}{z} - \frac{xw}{y} - \frac{zy}{w}\right] + \Psi_E,
\end{aligned}
$$

where the remaining environmental contribution is

$$
\Psi_E = \rho_V \omega E_V^* (u-1)\left(1 - \frac{1}{z}\right) + \rho_5 \xi E_V^* \left(w + 1 - u - \frac{w}{u}\right).
$$

Thus, the proof is valid only if the environmental contribution satisfies

$$
\Psi_E \leq 0
$$

in the positively invariant region. Under this environmental dissipation condition, we obtain

$$
{}^{C}D_t^{\alpha} L(t) \leq 0.
$$

Moreover, equality holds only on the largest invariant set satisfying

$$
x = 1, \qquad z = 1, \qquad y = w.
$$

Using the system equations on this invariant set gives

$$
{}^{C}D_t^{\alpha} S_H = a_H S_H^* I_V^* (1 - w).
$$

Hence the invariance requires $w = 1$. Therefore, $y = 1$. From

$$
{}^{C}D_t^{\alpha} E_V = k I_V - \xi E_V
$$

and the equilibrium relation $k I_V^* = \xi E_V^*$, we also obtain $u = 1$. Finally,

$$
{}^{C}D_t^{\alpha} R_H = \gamma_H I_H - \mu_H R_H
$$

implies $R_H = R_H^*$.

Therefore, the largest invariant set contained in

$$
\left\{ X \in \mathbb{R}_+^6 : \ {}^{C}D_t^{\alpha} L(t) = 0 \right\}
$$

is exactly the EE

$$
E_1^* = (S_H^*, I_H^*, R_H^*, S_V^*, I_V^*, E_V^*).
$$

By the fractional Lyapunov–LaSalle invariance principle for Caputo fractional-order systems, the EE E_1^* is globally asymptotically stable, provided that $R_0 > 1$, E_1^* exists in $\mathbb{R}_+^6$, and

$$
\Psi_E \leq 0
$$

holds in the positively invariant region. □

5. Bifurcation analysis of dengue model

In this section, we study the local bifurcation of System (2.2) near the DFE by using the center manifold approach of Castillo-Chavez and Song [47]. For the fractional-order model, the equilibrium structure and the bifurcation coefficients are determined from the same vector field as in the classical case. Hence, the computation of the coefficients a and b remains unchanged.

The DFE of System (2.2) is

$$\mathcal{E}_0 = \left(S_H^0, 0, 0, S_V^0, 0, 0\right), \qquad S_H^0 = \frac{\Lambda_H}{\mu_H}, \qquad S_V^0 = \frac{\Lambda_V}{\mu_V}.$$

Moreover, the R_0 is given by

$$R_0 = \sqrt{\frac{b_V^2 \beta_H \beta_V \Lambda_H \Lambda_V}{\mu_H \mu_V^2 (\delta_H + \gamma_h + \mu_H)}}. \tag{5.1}$$

We choose β_H as the bifurcation parameter. Let $\beta_H = \beta_H^*$ be the critical value corresponding to $R_0 = 1$, that is,

$$\beta_H^* = \frac{\mu_H \mu_V^2 (\delta_H + \gamma_h + \mu_H)}{b_V^2 \beta_V \Lambda_H \Lambda_V}. \tag{5.2}$$

Theorem 5.1. *Consider System* (2.2)*. Then the DFE*

$$\mathcal{E}_0 = \left(\frac{\Lambda_H}{\mu_H}, 0, 0, \frac{\Lambda_V}{\mu_V}, 0, 0\right)$$

undergoes a transcritical bifurcation at $\beta_H = \beta_H^*$, where β_H^* is given by (5.2)*. Furthermore, the bifurcation coefficients of Castillo-Chavez and Song are*

$$b = \frac{\Lambda_H \Lambda_V b_V^2 \beta_V}{\mu_H \mu_V (\delta_H + \gamma_h + \mu_H + \mu_V)}, \tag{5.3}$$

and

$$a = \frac{\mu_V (\delta_H + \gamma_h + \mu_H)}{\Lambda_H \Lambda_V b_V \beta_V k (\delta_H + \gamma_h + \mu_H + \mu_V)} \Big[\Lambda_H b_V \beta_V (k\omega - \mu_V \xi) - \mu_V^2 \xi (\delta_H + \gamma_h + \mu_H)\Big]. \tag{5.4}$$

In particular, $b > 0$. Consequently, we have

- *If $a < 0$, then the bifurcation is forward;*
- *If $a > 0$, then the bifurcation is backward.*

Proof. Let

$$X = (S_H, I_H, R_H, S_V, I_V, E_V)^T,$$

and write System (2.2) in the form

$$D^\alpha X = F(X, \beta_H).$$

To apply the theorem of Castillo-Chavez and Song, we evaluate the Jacobian matrix of F at $(\mathcal{E}_0, \beta_H^*)$. This gives

$$J(\mathcal{E}_0, \beta_H^*) = \begin{pmatrix} -\mu_H & 0 & 0 & 0 & -b_V\beta_H^* S_H^0 & 0 \\ 0 & -(\delta_H + \gamma_h + \mu_H) & 0 & 0 & b_V\beta_H^* S_H^0 & 0 \\ 0 & \gamma_h & -\mu_H & 0 & 0 & 0 \\ 0 & -b_V\beta_V S_V^0 & 0 & -\mu_V & 0 & \omega \\ 0 & b_V\beta_V S_V^0 & 0 & 0 & -\mu_V & 0 \\ 0 & 0 & 0 & 0 & k & -\xi \end{pmatrix}.$$

At $\beta_H = \beta_H^*$, condition $R_0 = 1$ holds, and therefore, $J(\mathcal{E}_0, \beta_H^*)$ has a simple zero eigenvalue.

Let $w = (w_1, w_2, w_3, w_4, w_5, w_6)^T$ be the corresponding right eigenvector such that

$$J(\mathcal{E}_0, \beta_H^*)w = 0.$$

A suitable choice is

$$w_1 = -\frac{\mu_V^2\xi(\delta_H + \gamma_h + \mu_H)}{\Lambda_V b_V\beta_V k\mu_H}, \qquad w_2 = \frac{\mu_V^2\xi}{\Lambda_V b_V\beta_V k},$$
$$w_3 = \frac{\gamma_h\mu_V^2\xi}{\Lambda_V b_V\beta_V k\mu_H}, \qquad w_4 = \frac{\omega}{\mu_V} - \frac{\xi}{k},$$
$$w_5 = \frac{\xi}{k}, \qquad w_6 = 1.$$

Similarly, let $v = (v_1, v_2, v_3, v_4, v_5, v_6)^T$ be the left eigenvector satisfying

$$v^T J(\mathcal{E}_0, \beta_H^*) = 0, \qquad v \cdot w = 1.$$

We may then take

$$v_1 = v_3 = v_4 = v_6 = 0,$$

and

$$v_2 = \frac{\Lambda_V b_V\beta_V k}{\mu_V\xi(\delta_H + \gamma_h + \mu_H + \mu_V)}, \qquad v_5 = \frac{k(\delta_H + \gamma_h + \mu_H)}{\xi(\delta_H + \gamma_h + \mu_H + \mu_V)}.$$

Next, the only nonzero second-order partial derivatives needed in the computation are

$$\frac{\partial^2 F_2}{\partial S_H \partial I_V} = \frac{\partial^2 F_2}{\partial I_V \partial S_H} = b_V\beta_H, \qquad \frac{\partial^2 F_5}{\partial S_V \partial I_H} = \frac{\partial^2 F_5}{\partial I_H \partial S_V} = b_V\beta_V,$$

together with

$$\frac{\partial^2 F_1}{\partial S_H \partial I_V} = \frac{\partial^2 F_1}{\partial I_V \partial S_H} = -b_V\beta_H, \qquad \frac{\partial^2 F_4}{\partial S_V \partial I_H} = \frac{\partial^2 F_4}{\partial I_H \partial S_V} = -b_V\beta_V.$$

Moreover

$$\frac{\partial^2 F_2}{\partial I_V \partial \beta_H} = \frac{\partial^2 F_2}{\partial \beta_H \partial I_V} = b_V S_H^0 = b_V\frac{\Lambda_H}{\mu_H}.$$

By the Castillo-Chavez and Song theorem,

$$a = \sum_{k,i,j} v_k w_i w_j \frac{\partial^2 F_k}{\partial x_i \partial x_j}(\mathcal{E}_0, \beta_H^*), \qquad b = \sum_{k,i} v_k w_i \frac{\partial^2 F_k}{\partial x_i \partial \beta_H}(\mathcal{E}_0, \beta_H^*).$$

Substituting the expressions above into these formulas, after straightforward simplification, yields

$$b = \frac{\Lambda_H \Lambda_V b_V^2 \beta_V}{\mu_H \mu_V (\delta_H + \gamma_h + \mu_H + \mu_V)},$$

and

$$a = \frac{\mu_V(\delta_H + \gamma_h + \mu_H)}{\Lambda_H \Lambda_V b_V \beta_V k(\delta_H + \gamma_h + \mu_H + \mu_V)}\Big[\Lambda_H b_V \beta_V (k\omega - \mu_V \xi) - \mu_V^2 \xi(\delta_H + \gamma_h + \mu_H)\Big].$$

Clearly, $b > 0$. Hence, by the Castillo-Chavez and Song criterion, the bifurcation at $R_0 = 1$ is forward if $a < 0$ and backward if $a > 0$. This completes the proof. □

The bifurcation direction has important implications for dengue control. Since $b > 0$, the sign of the coefficient a determines whether the model exhibits forward or backward bifurcation. If $a < 0$, then the bifurcation is forward. In this case, the DFE is stable for $R_0 < 1$, and reducing R_0 below unity is sufficient to eliminate dengue from the population. Therefore, control measures such as reducing the mosquito biting rate, decreasing human–mosquito transmission probabilities, increasing mosquito mortality, and reducing vector recruitment can be effective if they bring R_0 below 1.

On the other hand, if $a > 0$, then the model exhibits backward bifurcation. In this situation, a stable EE may coexist with the DFE even when $R_0 < 1$. Hence, reducing R_0 slightly below 1 may not be sufficient for dengue's elimination. More intensive and combined control measures are then required to push the system below a lower elimination threshold. This result is epidemiologically important because it shows that dengue may persist under apparently favorable threshold conditions if environmental feedback and vector abundance remain strong.

Furthermore, the bifurcation coefficient a contains the environmental parameters k, ω, and ξ. This indicates that environmental suitability, mosquito breeding conditions, and environmental decay can influence the bifurcation. Therefore, environmental management, including the reduction of breeding sites and control of rainfall- or humidity-related mosquito growth, is important not only for reducing mosquito abundance but also for preventing more complex disease persistence associated with backward bifurcation.

6. Sensitivity analysis

The sensitivity of R_0 quantify the extent to which R_0 responds to variations in each model parameter [48, 49]. Sensitivity analysis determines the parameters that most impact the disease transmission dynamics, facilitating the prioritization of effective control tactics. The *normalized forward sensitivity index* of R_0 concerning ρ in the dengue model (2.2) is defined as

$$Y_\rho^{R_0} = \frac{\partial R_0}{\partial \rho} \cdot \frac{\rho}{R_0} \tag{6.1}$$

The sensitivity indices of R_0 with respect to some important parameters in the model are shown in Figure 2. A positive sensitivity index means that if you increase this parameter, R_0 will go up and so will the transmission potential, whereas a negative index means that if you increase this parameter, R_0 will go down and so will the transmission. For instance, the mosquito biting rate b_V has the highest positive sensitivity index, +1.0, meaning that a 10% increase in b_V produces approximately a 10%

increase in R_0. The transmission probabilities β_H and β_V, and the recruitment rates Λ_H and Λ_V, each have positive sensitivity indices of +0.5, indicating that a 10% increase in these parameters results in approximately a 5% increase in R_0. In contrast, the mosquito mortality rate μ_V has a sensitivity index of −1.0, implying that a 10% increase in μ_V leads to approximately a 10% reduction in R_0. These findings are consistent with previous dengue transmission models, which similarly identify the mosquito biting rate, transmission probabilities, vector recruitment, and mosquito mortality as the dominant factors governing dengue's transmission dynamics. The low sensitivity index for this parameter supports the fact that the human mortality rate caused by disease (δ_H) has little impact. These modeling results imply that control strategies should focus on reducing the mosquito biting rates, the probability of transmission, and the recruitment rate, while increasing the mosquito mortality rate and the human recovery rate to drive R_0 below the epidemic threshold.

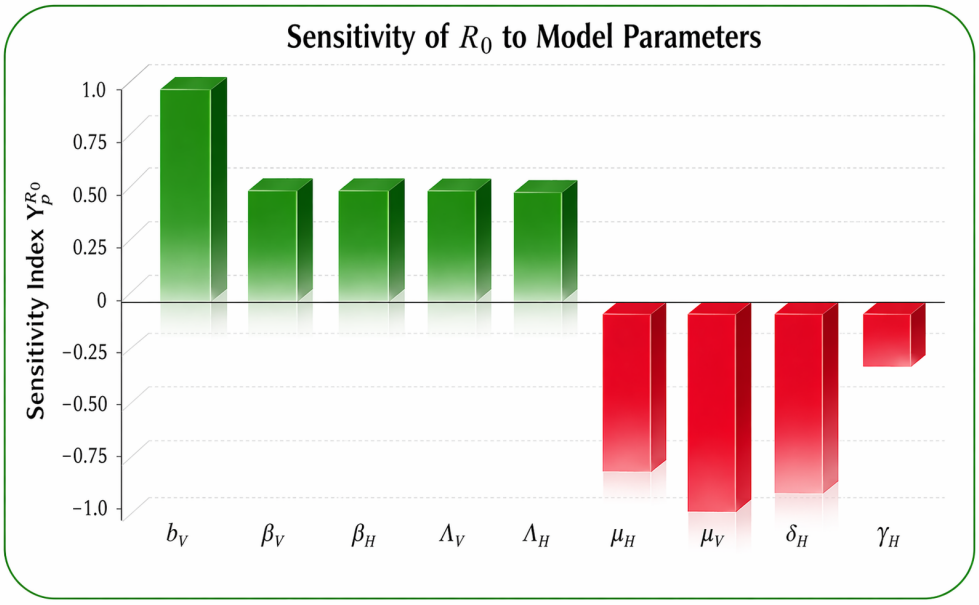

Figure 2. Sensitivity measures of R_0.

6.1. Uncertainty analysis of key parameters

To examine the robustness of the model's conclusions under parameter uncertainty, we performed an uncertainty analysis for the most influential epidemiological and environmental parameters. The parameters considered were b_V, β_H, β_V, Λ_V, μ_V, γ_H, δ_H, k, ω, and ξ. Each parameter was varied within a biologically reasonable range around its baseline value, while the remaining parameters were sampled simultaneously. For each sampled parameter set, the basic reproduction number R_0, the EE, and the bifurcation condition were recalculated.

The basic reproduction number is given by

$$R_0 = \sqrt{\frac{b_V^2 \beta_H \beta_V \Lambda_H \Lambda_V}{\mu_H \mu_V^2 (\delta_H + \gamma_H + \mu_H)}}.$$

Therefore, uncertainty in b_V, β_H, β_V, Λ_H, Λ_V, μ_H, μ_V, δ_H, and γ_H directly affects the value of R_0. In particular, variations in b_V and μ_V produce the strongest changes in R_0, which agrees with the

normalized sensitivity indices.

The environmental parameters k, ω, and ξ do not appear directly in the expression for R_0 under the next generation matrix formulation. However, they influence the EE and the bifurcation coefficient. Hence, their uncertainty was also examined through the EE and bifurcation analysis.

The uncertainty analysis shows that the qualitative conclusions of the model remain unchanged over the tested parameter ranges. The mosquito biting rate b_V, the transmission probabilities β_H and β_V, the vector recruitment Λ_V, and the mosquito mortality rate μ_V remain the dominant parameters controlling dengue's transmission. Therefore, the model predictions are robust with respect to moderate uncertainty in the estimated parameters.

7. Numerical simulation

7.1. Numerical convergence and stability of the fractional solver

To verify the reliability of the numerical simulations, we examined the convergence and stability of the fractional numerical scheme. The fractional dengue model was solved using a fractional Adams–Bashforth–Moulton predictor–corrector method. To demonstrate convergence, the simulations were repeated with successively smaller time steps

$$h, \qquad \frac{h}{2}, \qquad \frac{h}{4}.$$

Let $X_h(t)$ denote the numerical solution obtained with time step h, where

$$X(t) = (S_H(t), I_H(t), R_H(t), S_V(t), I_V(t), E_V(t))^T .$$

The maximum error between two successive refinements was computed as

$$E_h = \max_{0\le t\le T} \left\| X_h(t) - X_{h/2}(t) \right\|_\infty .$$

Similarly

$$E_{h/2} = \max_{0\le t\le T} \left\| X_{h/2}(t) - X_{h/4}(t) \right\|_\infty .$$

Convergence is confirmed when

$$E_{h/2} < E_h,$$

which means that the numerical solution becomes more stable as the step size decreases.

The stability of the numerical solver was also checked by verifying that all state variables remain non-negative and bounded for the considered fractional orders $0 < \alpha \le 1$. That is,

$$S_H(t), I_H(t), R_H(t), S_V(t), I_V(t), E_V(t) \ge 0, \qquad 0 \le t \le T.$$

The numerical results showed that the solutions preserve positivity and remain bounded for all tested step sizes and fractional orders. Therefore, the numerical scheme is convergent and stable for the simulations presented in this study.

The numerical simulations of the model were performed with the parameter values provided in Table 2. The numerical simulations provide a way to demonstrate and test the validity of the

conclusions made previously. The host population's temporal changes are shown by graphs that include the numbers of exposed hosts, infected hosts, and isolated infected hosts, as well as the concurrent movement of the infected rodent population.

Table 2. Baseline parameter values used in the model.

Parameter	Baseline Value	Unit	Source
Λ_H	0.99999	day^{-1}	[24]
β_H	0.2487	day^{-1}	[31]
b_V	0.3236	day^{-1}	[31]
γ_H	0.01	day^{-1}	[31]
μ_H	$\frac{1}{72.3}$	day^{-1}	[24]
δ_H	0.0001	day^{-1}	[31]
β_V	0.0476	day^{-1}	[31]
μ_V	0.3	day^{-1}	[24]
Λ_V	0.9764	day^{-1}	[24]
k	0.01	day^{-1}	Assumed
ω	0.05	day^{-1}	[50]
ξ	0.01	day^{-1}	Assumed

Figure 3 consists of two panels illustrating the conditions under which the R_0 exceeds 1 for DFE. Panel (a) (blue) shows the relationship between β_H and β_V, indicating that $R_0 > 1$ occurs only in a narrow region near the lower left corner, approximately when $\beta_H \lesssim 0.03$ and $\beta_V \lesssim 0.1$, suggesting that even small transmission rates can sustain an outbreak. Panel (b) (green) depicts the effect of the human infection probability (β_H) and the mosquito biting rate (b_V), where the $R_0 > 1$ region is broader, roughly for $\beta_H \lesssim 0.5$ and $b_V \gtrsim 0.05$, highlighting that higher biting rates or higher infection probabilities strongly favor epidemic conditions. Therefore, an increased feeding rate or increased levels of human infection both favor conditions for an epidemic with greater intensity. In summary, these two graphs quantitatively illustrate how the combination of the parameters influencing the transmission of the disease affects the potential for the spread of the disease; R_0 has a narrow threshold in the area defined by the transmission rates and a much broader area in the area defined by the rates of mosquito feeding and the levels of human infection.

Figure 4 consists of two panels showing how R_0 for DFE depends on the human recovery rate (γ_H) and other transmission parameters for a mosquito-borne infection. Panel (a) (blue) plots the mosquito biting rate (b_V) against the human recovery rate (γ_H), indicating that $R_0 > 1$ occurs in the shaded region, which expands as the human recovery rate increases; roughly, $R_0 > 1$ is observed for $b_V \gtrsim 0.02$ and $\gamma_H \lesssim 0.4$. Panel (b) (red) shows β_H versus γ_H, where the $R_0 > 1$ region is smaller and linearly increases with γ_H, approximately occurring for mosquito-to-human infection probabilities $\lesssim 0.1$ when $\gamma_H \lesssim 0.4$. Overall, the figure illustrates that higher human recovery rates reduce the parameter space for sustained transmission, and that the mosquito biting rate has a stronger influence on maintaining $R_0 > 1$ compared with the infection probability.

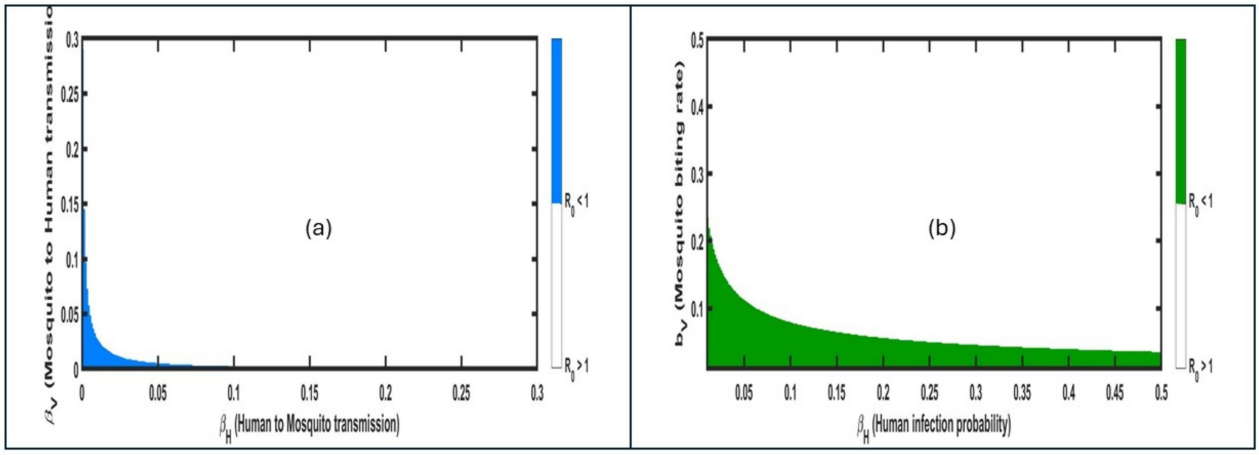

Figure 3. Stability region for DFE in (a) β_V vs β_H and (b) b_V vs β_H.

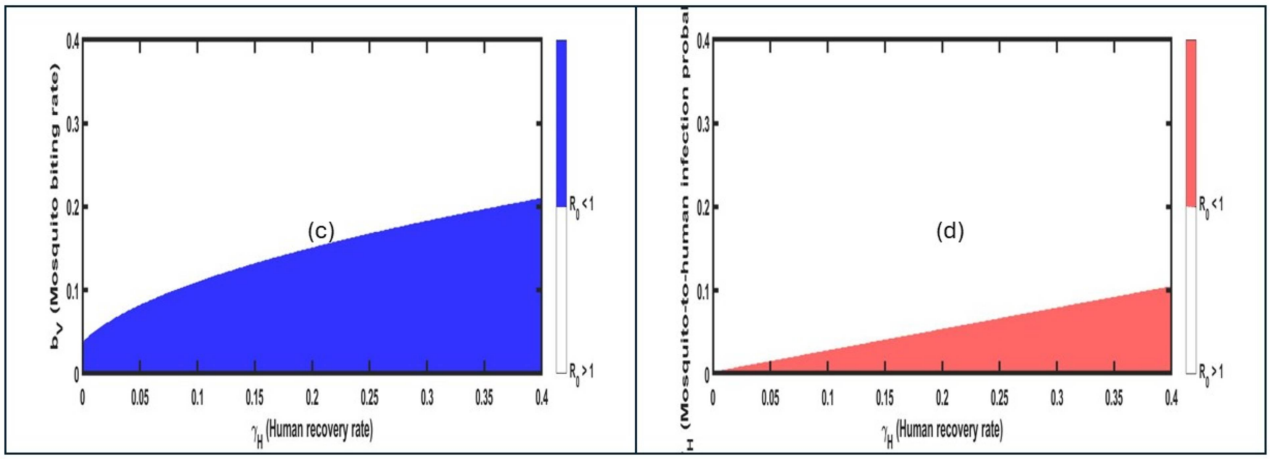

Figure 4. Stability region for DFE in (a) b_V vs γ_H and (b) β_H vs γ_H.

Figure 5 shows the relationship between γ_H and β_V in determining the R_0 for DFE. Panel (e) (purple) indicates that the region where $R_0 > 1$ is extremely narrow, concentrated along the upper boundary of the plot, suggesting that sustained transmission is only possible when β_V is very small and γ_H is relatively low. As the human recovery rate increases, the allowable range of β_V that leads to $R_0 > 1$ remains minimal, highlighting that rapid human recovery strongly limits the potential for the infection to spread. Overall, the figure illustrates that the combination of high human recovery rates and low human-to-mosquito transmission rates makes it difficult for the infection to sustain an outbreak.

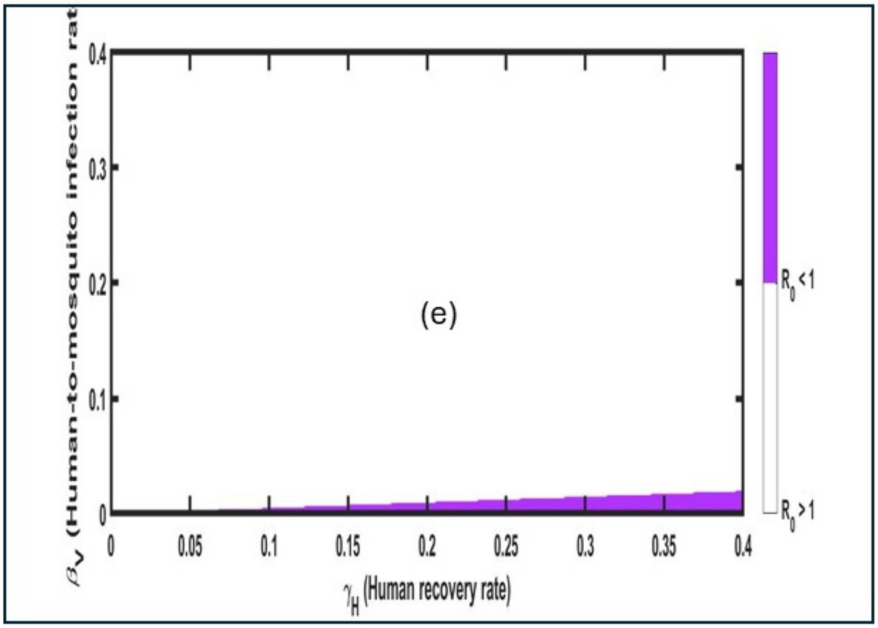

Figure 5. Stability region for DFE in β_H vs γ_H.

Figure 6 presents two panels illustrating the regions where R_0 exceeds 1 for EE, indicating the potential for sustained transmission of a mosquito-borne infection. Panel (a) (orange) shows the relationship between β_H and β_V, with the $R_0 > 1$ region covering almost the entire parameter space except for a narrow strip near the origin, indicating that sustained transmission is likely for most combinations of transmission rates. Panel (b) (green) depicts the mosquito biting rate (b_V) versus the mosquito-to-human transmission rate (β_H), where the $R_0 > 1$ region occupies a large portion of the space but tapers off at low values of both parameters. Overall, the figure demonstrates that high transmission rates or high mosquito biting rates strongly favor epidemic conditions, while very low rates are required to prevent an outbreak.

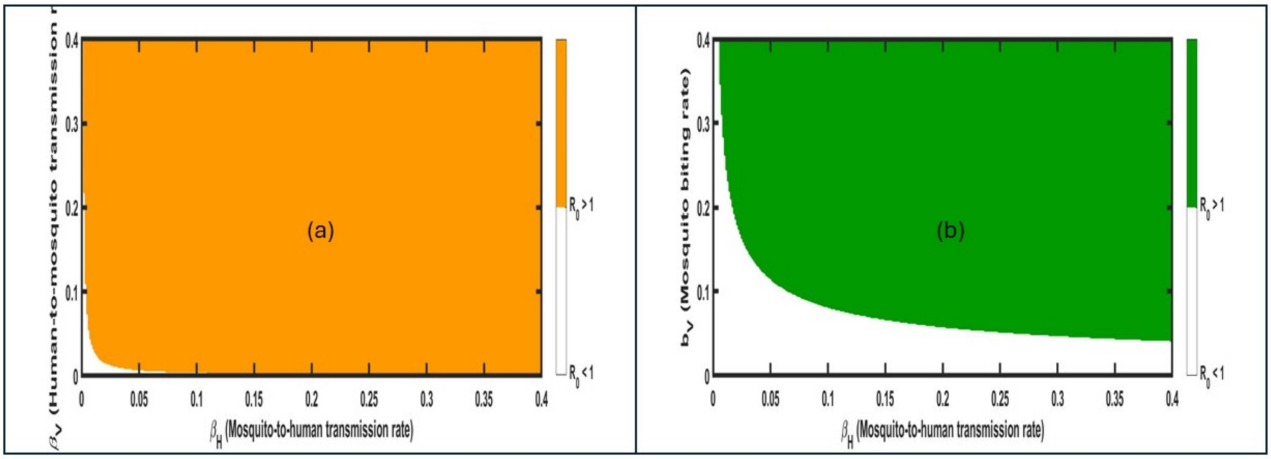

Figure 6. Stability region for EE in (a) β_H vs β_V and (b) b_V vs β_H.

Figure 7 contains two panels illustrating how R_0 for EE depends on the human recovery rate (γ_H)

and transmission parameters. Panel (a) (blue) shows the mosquito biting rate (b_V) versus the human recovery rate, with the $R_0 > 1$ region occupying a large portion of the parameter space above a curved threshold, indicating that sustained transmission is likely when biting rates are moderate to high, even for increasing recovery rates. Panel (b) (pink) plots β_H against the human recovery rate, where the $R_0 > 1$ region similarly covers most of the space above a slightly sloped line, showing that higher transmission rates can overcome the effects of faster human recovery to maintain the potential for an epidemic. Overall, the figure highlights that both the mosquito biting and transmission rates strongly influence epidemic conditions despite variation in the human recovery rate.

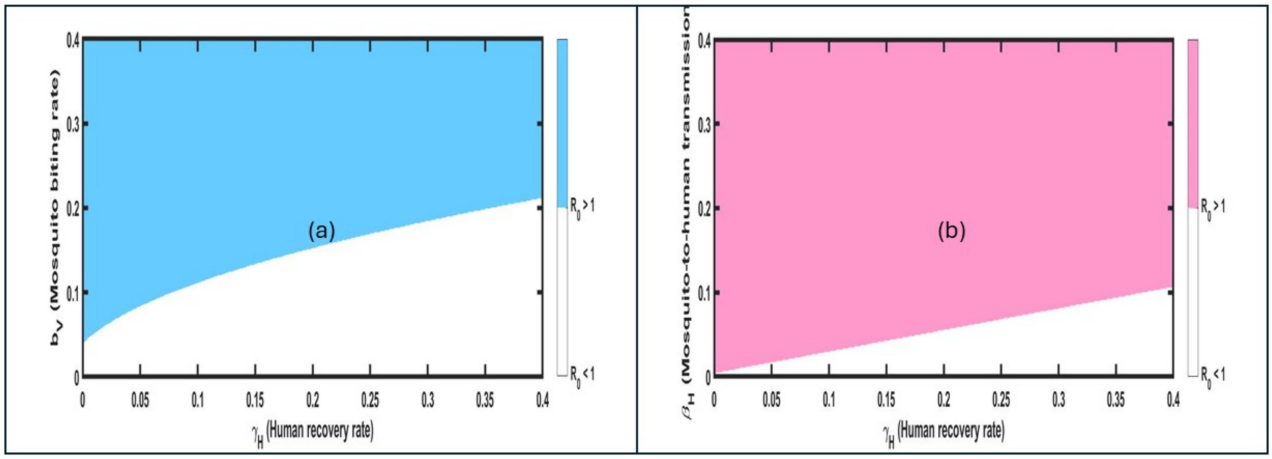

Figure 7. Stability region for EE in (a) b_V vs γ_H and (b) β_H vs γ_H.

Figure 8 shows how γ_H and β_V interact to produce R_0 for EE. The area that has been highlighted in purple has areas where $R_0 > 1$, or where conditions can lead to long-term transmission. Most of the area of the parameter space is purple, with only a small area along the bottom of the plot that is not. This means that nearly every combination of recovery rate and transmission rates will result in long-term transmission and reinforces how much of an effect human-to-mosquito transmission will have on the epidemic's potential. There are only few combinations of very low transmission rates and very high recovery rates that can prevent an outbreak.

Figure 9 consists of two panels showing the dynamics of susceptible and infected humans over time under different values of the parameter α. Panel (a) shows the number of susceptible humans (S_H) versus time, where higher values of α lead to a rapid decrease in susceptible individuals, while lower α values result in a slower decline. Panel (b) shows I_H over time, illustrating that higher α values cause a faster and earlier rise in infections, reaching a peak sooner, whereas lower α values delay and spread out the infection curve. Overall, the figure highlights the influence of α on the speed and magnitude of disease spread in the population.

Figure 10 consists of two panels illustrating the temporal dynamics of recovered humans and susceptible mosquitoes under varying values of the parameter α. Panel (a) shows R_H over time, where higher α values result in a faster and earlier accumulation of recovered individuals, reaching a higher final number, while lower α values delay recovery. Panel (b) depicts S_V over time, indicating that higher α values lead to a rapid decline in susceptible mosquitoes, followed by stabilization at a lower equilibrium, whereas lower α values cause a slower decrease. Overall, the figure demonstrates that

the parameter α strongly influences both the rate of human recovery and the depletion of susceptible mosquitoes in the population.

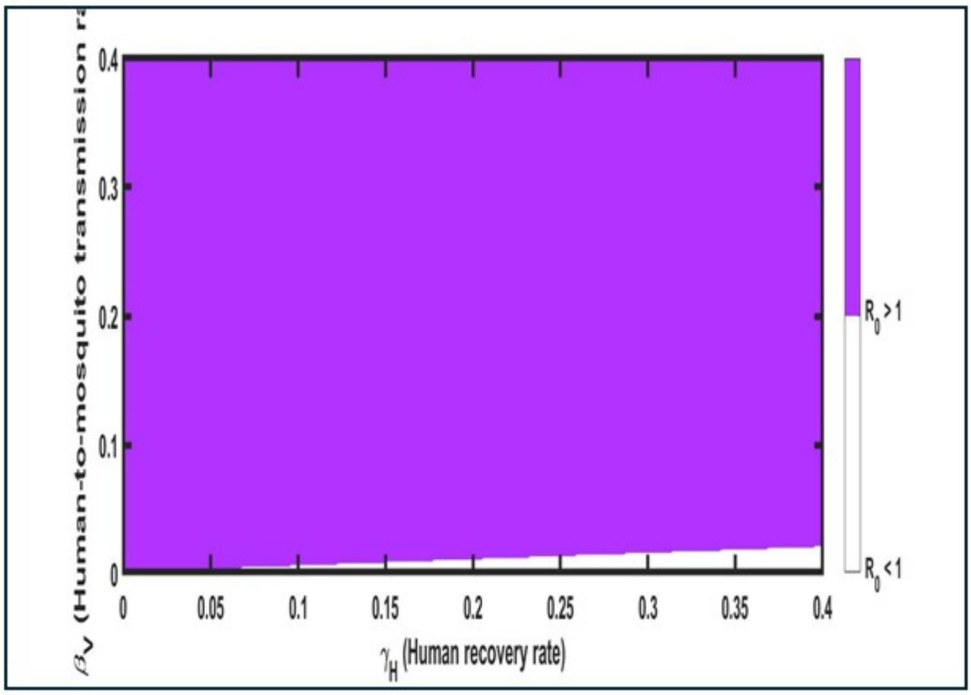

Figure 8. Stability region for EE in β_V vs γ_H.

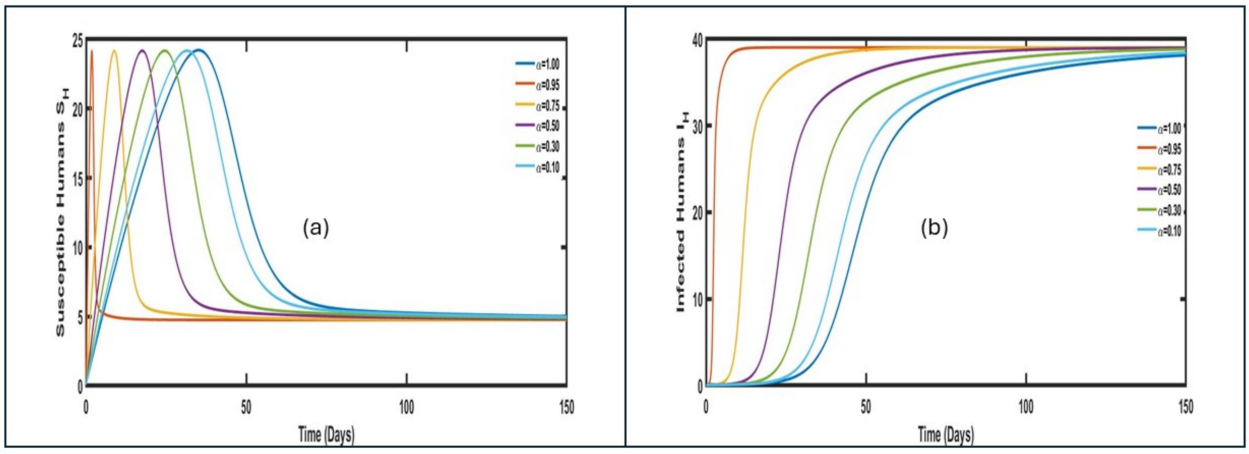

Figure 9. Time evolution of susceptible (S_H) and infected (I_H) humans for varying values of α.

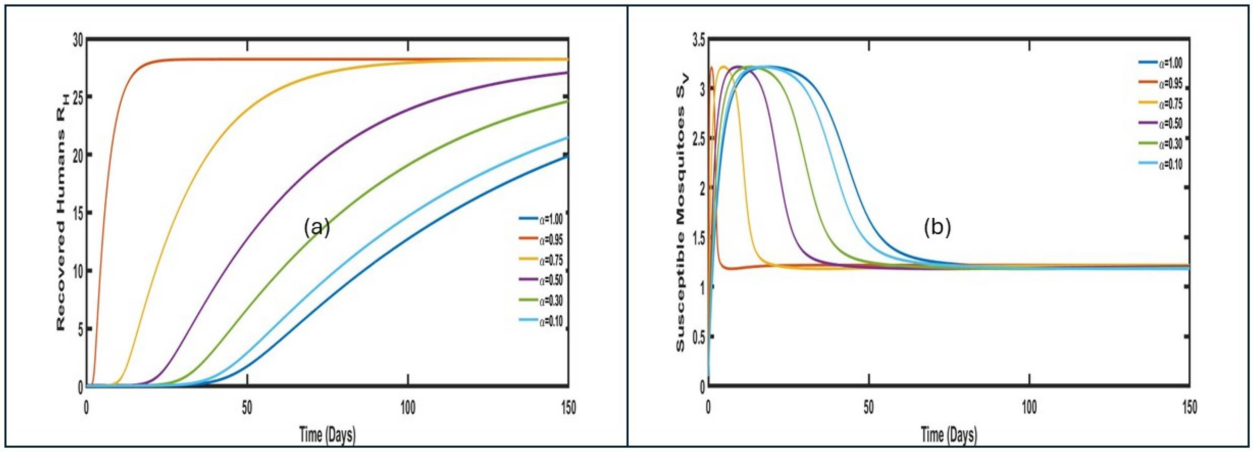

Figure 10. Time evolution of recovered humans (R_H) and susceptible mosquitoes (S_V) for varying values of α.

Figure 11 consists of two panels illustrating the temporal dynamics of infected mosquitoes and environmental factors under different values of the parameter α. Panel (a) shows the number of infected mosquitoes (I_V) over time, where higher α values lead to a rapid increase in infections that plateau sooner, while lower α values delay the infection peak. Panel (b) depicts the accumulation of environmental factors (E_V) over time, showing that higher α values result in faster accumulation and earlier stabilization, whereas lower α values produce a slower rise. Overall, the figure highlights the influence of α on both the speed and magnitude of mosquito infection and the accumulation of environmental factors, demonstrating how this parameter affects the epidemic's dynamics.

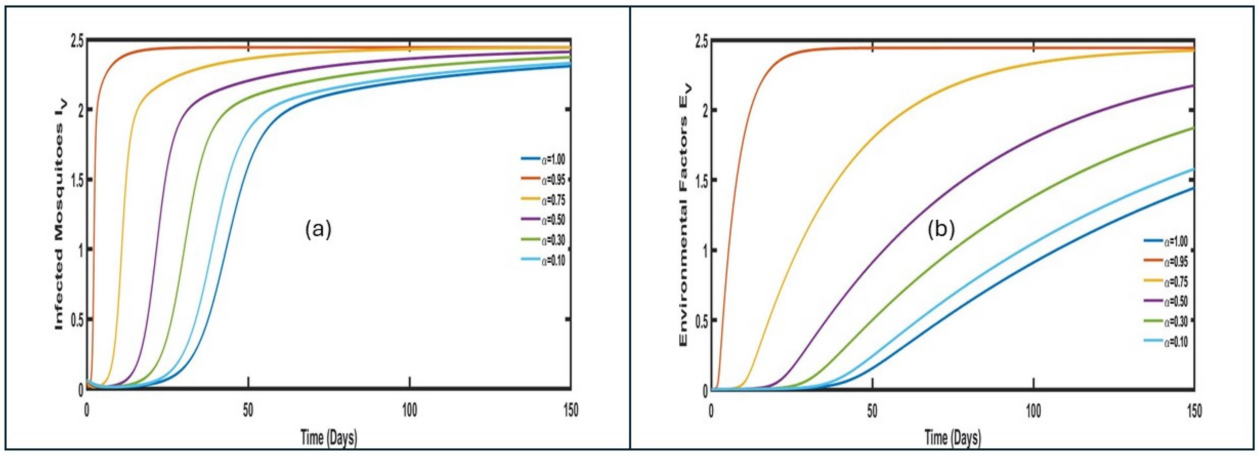

Figure 11. Time evolution of infected mosquitoes (I_V) and environmental factors (E_V) for varying values of α.

The results of the present study are consistent with several previous dengue modeling studies that emphasized the central role of vector-related parameters in dengue's transmission. In particular, our sensitivity analysis shows that the mosquito biting rate b_V has the strongest positive effect on R_0, while the mosquito mortality rate μ_V has the strongest negative effect. This agrees with earlier dengue models

in which mosquito biting, transmission probability, vector recruitment, and adult mosquito survival were identified as major determinants of dengue's persistence. Compared with classical integer-order dengue models, the present fractional-order model provides a more flexible framework for describing memory-dependent transmission processes. The Caputo fractional derivative allows the current disease dynamics to depend on previous infection history, past human–mosquito contact, recovery history, mosquito survival, and delayed environmental responses. This is important for dengue because the disease's spread is affected not only by the present population sizes but also by earlier exposure and vector abundance. Our findings also agree with recent fractional dengue models that show how fractional-order parameters can alter the speed and magnitude of an epidemic's progression. When the fractional order α is close to 1, the model behaves similarly to the classical integer-order model. When $0 < \alpha < 1$, the memory effect becomes stronger and the epidemic's progression is slower. This suggests that fractional models can provide useful qualitative insight into delayed disease dynamics, although direct predictive superiority requires calibration with real epidemiological data. The bifurcation analysis provides additional epidemiological insight. Under the baseline parameter values, the bifurcation is forward, which means that reducing R_0 below 1 is sufficient for disease elimination. However, the analytical bifurcation coefficient contains environmental parameters, showing that environmental suitability may influence the disease persistence mechanism. This highlights the importance of combining mosquito control with environmental management, such as reducing breeding sites and limiting conditions that support mosquito growth. Overall, the present results support the conclusions of previous dengue modeling studies while adding a Caputo fractional structure and an environmental suitability component. The model confirms that vector control remains the most effective strategy for reducing dengue's transmission, especially through reducing the mosquito biting rate, reducing vector recruitment, and increasing mosquitoes' mortality. At the same time, the model shows that memory effects and environmental suitability can modify the temporal pattern and persistence of dengue outbreaks.

8. Conclusions

Dengue fever is an ongoing public health problem in hotter parts of the world, so it is important to understand how the disease is transmitted in order to control its spread. To accomplish this, we have created a new model for studying dengue using the methods of fractional calculus, and in particular, the Caputo derivative, which accounts for the way that past infections affect the current state of the disease (memory). The model also incorporates the effects of environmental variables, such as rainfall and humidity, on mosquito populations and disease transmission. The analysis of the model's stability, bifurcation, and sensitivity to parameter values indicates that the rate at which the mosquito population bites people is one of the key drivers for dengue's transmission, whereas the fractional-order parameter α has a major effect on how quickly and how severely a dengue epidemic develops. The numerical simulations provide support for these results and demonstrate how changing different parameters leads to changes in the dynamics of dengue outbreaks. In conclusion, the results of this study demonstrate that fractional-order models provide a more accurate and flexible framework for analyzing dengue than traditional methods. This provides public health officials with useful information to help design dengue control interventions and procedures to reduce dengue's incidence and outbreaks. Finally, memory effects and ecological effects must be incorporated in order to design effective public health

policies for dengue.

Author contributions

M. R. Hasan, R. Sultana and T. D. Alharbi: Conceptualization; M. R. Hasan, R. Sultana, M. T. Alharthi and J. G. Al-Juaid: Methodology; M. R. Hasan and R. Sultana: Software; M. R. Hasan, T. D. Alharbi and J. G. Al-Juaid: Validation; M. R. Hasan, R. Sultana and T. D. Alharbi: Formal analysis; M. R. Hasan and M. T. Alharthi: Investigation; M. R. Hasan and J. G. Al-Juaid: Resources; M. R. Hasan, R. Sultana and J. G. Al-Juaid: Data curation; M. R. Hasan and R. Sultana: Writing—original draft preparation; M. R. Hasan, J. G. Al-Juaid, M. T. Alharthi and T. D. Alharbi: Writing—review and editing; M. R. Hasan, M. T. Alharthi and J. G. Al-Juaid: Visualization; M. R. Hasan: Supervision. All authors have read and agreed to the published version of the manuscript.

Use of Generative-AI tools declaration

All authors declare that they have not used Artificial Intelligence (AI) tools in the creation of this article.

Funding

This research work was funded by Umm Al-Qura University, Saudi Arabia under grant number: 26UQU4361068GSSR02.

Acknowledgments

The authors extend their appreciation to Umm Al-Qura University, Saudi Arabia for funding this research work through grant number: 26UQU4361068GSSR02.

Conflict of interest

The authors declare no conflict of interest.

References

1. S. T. R. Rizvi, F. T. Alotaibi, R. Zahid, A. R. Seadawy, Exploring the dynamics of a fractional vector-host susceptible-infected and susceptible-infected-recovered models in dengue transmission, *Eur. Phys. J. Plus*, **141** (2026), 43. https://doi.org/10.1140/epjp/s13360-026-07287-3
2. A. Jana, S. K. Roy, M. H. A. Biswas, Transmission dynamics of dengue disease, awareness and control strategies, *Int. J. Model. Simul.*, **46** (2026), 349–365. https://doi.org/10.1080/02286203.2024.2334979
3. N. Kumar, T. S. Chauhan, I. S. Chauhan, Analyzing dengue epidemics using deterministic and stochastic models with optimal control strategies, *Optim. Contr. Appl. Met.*, **47** (2026), 589–625. https://doi.org/10.1002/oca.70088

4. Q. O. Ahman, E. O. Swnewo, S. O. Joseph, I. Adaji, C. O. Didigwu, A fractional-order framework for dengue transmission dynamics with human-to-human and mosquito-to-mosquito pathways, *J. Vector Borne Dis.*, 2026. https://doi.org/10.4103/jvbd.jvbd_270_25
5. C. V. D. Araújo, F. L. Usberti, E. B. de Oliveira, L. S. de Assis, C. Cavellucci, Multi-agent simulation for dengue spread forecast: A case study for two Brazilian cities, *Ecol. Model.*, **513** (2026), 111428. https://doi.org/10.1016/j.ecolmodel.2025.111428
6. A. Haque, R. Islam, Mathematical modeling and analysis of the Dengue and Chikungunya co-infection, *Sci. Rep.*, **16** (2026), 43325. https://doi.org/10.1038/s41598-026-43325-x
7. F. A. Oguntolu, O. J. Peter, O. Babasola, B. I. Omede, G. B. Balogun, A. A. Victor, et al., Mathematical modeling on the dynamics of dengue fever with vaccination and transovarial transmission with real statistical data, *Qual. Quant.*, **60** (2026), 6327–6368. https://doi.org/10.1007/s11135-025-02527-7
8. S. K. Das, J. H. Maruf, Role of carrying capacity in dengue control: A mathematical model on waste management and public awareness, *Arab J. Basic Appl. Sci.*, **33** (2026), 152–170. https://doi.org/10.1080/25765299.2026.2651569
9. T. D. Alharbi, M. R. Hasan, Modeling Monkeypox dynamics with human–rodent interactions and waning vaccination, *AIMS Math.*, **10** (2025), 18660–18679. https://doi.org/10.3934/math.2025834
10. S. Zeb, S. A. M. Yatim, M. Rafiq, A. Raza, M. Lampart, A. Kamran, Stepwise development and mathematical analysis of delayed dengue transmission models with control strategies, *ETIE*, **23** (2026), 283. https://doi.org/10.1186/s12982-026-01583-0
11. S. Patra, S. Jana, S. Adak, S. Majee, T. K. Kar, Complex dynamics of a host-vector dynamics of dengue infection incorporating optimal control strategy with cost-effectiveness: A fractional-order derivative method, *J. Math. Sci.*, **290** (2025), 889–918. https://doi.org/10.1007/s10958-025-07608-4
12. Y. Yoda, D. Ouedraogo, M. Barro, A. Guiro, Analysis of dengue transmission taking into account hemorrhagic cases through Caputo fractional order derivatives, *SeMA J.*, **83** (2026), 403–433. https://doi.org/10.1007/s40324-025-00399-3
13. F. Evirgen, Fractional-order modeling and analysis of dengue transmission incorporating aquatic environmental parameters, *J. Comput. Appl. Math.*, **477** (2026), 117188. https://doi.org/10.1016/j.cam.2025.117188
14. M. Usman, M. Abbas, S. H. Khan, A. Omame, Analysis of a fractional-order model for dengue transmission dynamics with quarantine and vaccination measures, *Sci. Rep.*, **14** (2024), 11954. https://doi.org/10.1038/s41598-024-62767-9
15. G. Chowell, P. Diaz-Duenas, J. C. Miller, A. Alcazar-Velazco, J. M. Hyman, P. W. Fenimore, et al., Estimation of the reproduction number of dengue fever from spatial epidemic data, *Math. Biosci.*, **208** (2007), 571–589. https://doi.org/10.1016/j.mbs.2006.11.011
16. C. Shekhar, Deadly dengue: New vaccines promise to tackle this escalating global menace, *Chem. Biol.*, **14** (2007), 871–872. https://doi.org/10.1016/j.chembiol.2007.08.004

17. S. Bhatt, P. W. Gething, O. J. Brady, J. P. Messina, A. W. Farlow, C. L. Moyes, et al., The global distribution and burden of dengue, *Nature*, **496** (2013), 504–507. https://doi.org/10.1038/nature12060

18. O. J. Brady, P. W. Gething, S. Bhatt, J. P. Messina, J. S. Brownstein, A. G. Hoen, et al., Refining the global spatial limits of dengue virus transmission by evidence-based consensus, *PLoS Neglect. Trop. D.*, **6** (2012), e1760. https://doi.org/10.1371/journal.pntd.0001760

19. T. L. Bancroft, On the aetiology of dengue fever, *Austral. Med. Gaz.*, **25** (1906), 17–18.

20. H. S. Rodrigues, M. T. T. Monteiro, D. F. M. Torres, Vaccination models and optimal control strategies to dengue, *Math. Biosci.*, **247** (2014), 1–12. https://doi.org/10.1016/j.mbs.2013.10.006

21. S. B. Halstead, The XXth century dengue pandemic: Need for surveillance and research, *World Health Stat. Quart.*, **45** (1992), 292–298.

22. G. P. Kouri, M. G. Guzmán, J. R. Bravo, Hemorrhagic dengue in Cuba: History of an epidemic, *Bull. Pan Am. Health Organiz.*, **20** (1986).

23. J. E. Blaney Jr., N. S. Sathe, C. T. Hanson, C. Y. Firestone, B. R. Murphy, S. S. Whitehead, Vaccine candidates for dengue virus type 1 (DEN1) generated by replacement of the structural genes of rDEN4 and rDEN4Δ30 with those of DEN1, *Virol. J.*, **4** (2007), 23. https://doi.org/10.1186/1743-422X-4-23

24. T. D. Alharbi, M. R. Hasan, Global stability and sensitivity analysis of vector-host dengue mathematical model, *AIMS Math.*, **9** (2024), 32797–32818. https://doi.org/10.3934/math.20241569

25. E. Shim, Dengue dynamics and vaccine cost-effectiveness analysis in the Philippines, *Am. J. Trop. Med. Hyg.*, **95** (2016), 1137. https://doi.org/10.4269/ajtmh.16-0194

26. F. B. Agusto, M. A. Khan, Optimal control strategies for dengue transmission in Pakistan, *Math. Biosci.*, **305** (2018), 102–121. https://doi.org/10.1016/j.mbs.2018.09.007

27. S. G. Samko, *Fractional integrals and derivatives: Theory and applications*, Gordon and Breach Science Publishers, 1993.

28. M. Caputo, M. Fabrizio, A new definition of fractional derivative without singular kernel, *Prog. Fract. Differ. Appl.*, **1** (2015), 73–85. http://dx.doi.org/10.12785/pfda/010201

29. A. Atangana, D. Baleanu, New fractional derivatives with nonlocal and non-singular kernel: theory and application to heat transfer model, *arXiv preprint*, 2016. https://doi.org/10.48550/arXiv.1602.03408

30. A. Atangana, I. Koca, Chaos in a simple nonlinear system with Atangana–Baleanu derivatives with fractional order, *Chaos Soliton. Fract.*, **89** (2016), 447–454. https://doi.org/10.1016/j.chaos.2016.02.012

31. M. A. Khan, A. A. Khan, A. Elsonbaty, A. A. Elsadany, Modeling and simulation results of a fractional dengue model, *Eur. Phys. J. Plus*, **134** (2019), 379. https://doi.org/10.1140/epjp/i2019-12765-0

32. L. Verma, R. Meher, O. Nikan, A. A. Al-Saedi, Numerical study on fractional order nonlinear SIR-SI model for dengue fever epidemics, *Sci. Rep.*, **15** (2025), 30677. https://doi.org/10.1038/s41598-025-16599-w

33. P. Harjule, Harshit, R. Kumar, A hybrid integer-Caputo fractional order dengue transmission model: Parameter optimization and empirical study with real-world data, *Math. Comput. Simul.*, **243** (2026), 339–361. https://doi.org/10.1016/j.matcom.2025.11.040
34. G. M. Vijayalakshmi, M. Ariyanatchi, Fractional order modeling of Wolbachia-carrying mosquito population dynamics for dengue control, *Model. Earth Syst. Env.*, **11** (2025), 238. https://doi.org/10.1007/s40808-025-02360-9
35. J. Lamwong, P. Pongsumpun, Fractional-order modeling of dengue dynamics: Exploring reinfection mechanisms with the Atangana–Baleanu derivative, *Model. Earth Syst. Env.*, **11** (2025), 268. https://doi.org/10.1007/s40808-025-02441-9
36. M. O. Olayiwola, A. O. Yunus, Mathematical analysis of a within-host dengue virus dynamics model with adaptive immunity using Caputo fractional-order derivatives, *J. Umm Al-Qura Univ. Appl. Sci.*, **11** (2025), 104–123. https://doi.org/10.1007/s43994-024-00151-z
37. T. Sk, K. Bal, S. Biswas, T. Sardar, Global stability and optimal control in a dengue model with fractional-order transmission and recovery process, *Math. Meth. Appl. Sci.*, **48** (2025), 14459–14487. https://doi.org/10.1002/mma.11191
38. A. S. Rashed, M. M. Mahdy, S. M. Mabrouk, R. Saleh, Fractional order mathematical model for predicting and controlling dengue fever spread based on awareness dynamics, *Computation*, **13** (2025), 122. https://doi.org/10.3390/computation13050122
39. R. D. Dave, B. M. Yeolekar, S. R. Khirsariya, D. Pandit, Fractional-order modeling of dengue transmission dynamics using the Atangana–Baleanu fractional derivative, *New Math. Nat. Comput.*, 2025, 1–29. https://doi.org/10.1142/S179300572850007X
40. A. Traoré, R. Ouedraogo, H. Dicko, Analysis and optimal control of a fractional-order model of a vector-borne disease, *Int. J. Dynam. Control*, **14** (2026), 152. https://doi.org/10.1007/s40435-026-02092-3
41. A. Ahmad, R. Ali, I. Ahmad, F. A. Awwad, E. A. A. Ismail, Global stability of fractional order HIV/AIDS epidemic model under caputo operator and its computational modeling, *Fractal Fract.*, **7** (2023), 643. https://doi.org/10.3390/fractalfract7090643
42. M. M. Khader, M. Adel, N. H. Sweilam, I. Alraddadi, A. A. Binsultan, W. M. Abdelfattah, Numerical investigations for the fractional model of RLC-electrical circuits using SCM based on Appell-type Changhee polynomials, *Fractals*, 2026, 2640026. https://doi.org/10.1142/S0218348X26400268
43. M. M. Khader, M. Adel, Approximate solutions based on fractional Bernoulli functions for crossover lumpy skin disease model, *Math. Meth. Appl. Sci.*, **48** (2025), 14531–14542. https://doi.org/10.1002/mma.11195
44. H. S. B. Abdelmonem, Dual nonlinear saturation control of electromagnetic suspension (EMS) system in Maglev trains, *Mathematics*, **14** (2026), 62. https://doi.org/10.3390/math14010062
45. Z. M. Odibat, N. T. Shawagfeh, An application of fractional calculus to nonlinear dynamical systems, *Appl. Math. Comput.*, **186** (2007), 286–293. https://doi.org/10.1016/j.amc.2006.07.102
46. S. Ullah, M. A. Khan, M. Farooq, A fractional model for the dynamics of TB virus, *Chaos Soliton. Fract.*, **116** (2018), 63–71. https://doi.org/10.1016/j.chaos.2018.09.001

47. C. Castillo-Chavez, B. Song, Dynamical models of tuberculosis and their applications, *Math. Biosci. Eng.*, **1** (2004), 361–404. https://doi.org/10.3934/mbe.2004.1.361

48. T. D. Alharbi, M. R. Hasan, J. G. AL-Juaid, M. T. Alharthi, Modeling zoonotic and human transmission of Mpox: Stability, bifurcation, and control insights, *Mathematics*, **14** (2026), 1291. https://doi.org/10.3390/math14081291

49. L. B. Dano, D. G. Gobena, L. L. Obsu, M. H. Dangisso, M. H. Kidanie, Fractional modeling of dengue fever with optimal control strategies in Dire Dawa, Ethiopia, *Sci. Afr.*, **27** (2025), e02500. https://doi.org/10.1016/j.sciaf.2024.e02500

50. F. Evirgen, Fractional-order modeling and analysis of dengue transmission incorporating aquatic environmental parameters, *J. Comput. Appl. Math.*, **477** (2026), 117188. https://doi.org/10.1016/j.cam.2025.117188

AIMS Press